Highlights

Paleoclimate and paleoecology of the latest Eocene Florissant flora of central Colorado, U.S.A.

Sarah E. Allen[1], Alexander J. Lowe[2,*], Daniel J. Peppe[3], Herbert W. Meyer[4]

- The uppermost Eocene Florissant Formation in Colorado preserves a diverse flora.
- The majority of morphotypes indicated a leaf lifespan of approximately one year.
- Mean annual temperature for Florissant was estimated to be 11.6 ± 3.3 °C.
- Mean annual precipitation was estimated at 740 +608/-334 $mm \cdot yr^{-1}$.
- Florissant provides key climate data just before the transition to the Oligocene.

Paleoclimate and paleoecology of the latest Eocene Florissant flora of central Colorado, U.S.A.

Sarah E. Allen[1], Alexander J. Lowe[2*], Daniel J. Peppe[3], Herbert W. Meyer[4]

[1]*Department of Biology, Penn State Altoona, 3000 Ivyside Park, Altoona, PA 16601 USA*

[2]*Department of Biology, University of Washington, 24 Kincaid Hall, Seattle, WA 98195 USA*

[3]*Terrestrial Paleoclimatology Research Group, Department of Geosciences, Baylor University, Waco, TX 76706, USA*

[4]*National Park Service, Florissant Fossil Beds National Monument, P.O. Box 185, Florissant, CO 80816, USA*

Corresponding author: E-mail address:* loweaj01@uw.edu

ABSTRACT

The uppermost Eocene Florissant Formation of central Colorado, U.S.A. contains a diverse flora and fauna preserved in lacustrine facies and represents a key episode in Earth history immediately preceding the Eocene-Oligocene boundary. Laminated shales contain impressions of non-monocot angiosperm leaves that were used to estimate paleoecological and paleoclimatic parameters using leaf physiognomic methods including: leaf mass per area (M_A), digital leaf physiognomy (DiLP), leaf margin analysis (LMA), and leaf area analysis (LAA). The majority (58%) of the morphotypes analyzed for M_A suggested a semi-evergreen leaf lifespan, whereas another 27% indicated a deciduous habit and 15% an evergreen habit. There was no significant relationship between M_A and insect damage based on a small subset of Florissant's leaves. Higher M_A values (~73% of leaves ≥ one-year lifespan), coupled with a tendency toward long and narrow leaf shapes and small leaf areas, indicate the existence of sclerophyllous vegetation. Using the global regression for mean annual temperature (MAT), the DiLP estimate of MAT was anomalously cold: 5.5 ± 4 °C. However, using a Northern Hemisphere regression the DiLP MAT estimate of 11.6 ± 3.3 °C was more plausible. Using DiLP, mean annual precipitation (MAP) was estimated at 740 +608/-334 mm·yr^{-1}, which supports dry conditions. Estimates for MAT and MAP using the univariate LMA and LAA methods overlapped within uncertainty of the DiLP results. In addition, those taxa classified as growing in wet areas (riparian) had significantly more teeth than non-riparian taxa. These paleoclimatic and paleoecological results suggest that outside the riparian forest, the Florissant flora sampled a seasonally dry temperate sclerophyllous shrubland to woodland, perhaps similar to modern chaparral forests, in the western interior of the U.S.A. just before the transition into the cooler Oligocene.

Keywords: digital leaf physiognomy; leaf area analysis; leaf margin analysis; leaf mass per area; leaf physiognomy; paleobotany

1. Introduction

The uppermost Eocene Florissant Formation (34.1 Ma; Evanoff et al., 2001) preserves a small freshwater lacustrine deposit in central Colorado, USA (Fig. 1). The ancient lake formed from the damming of a stream valley by a lahar (Evanoff et al., 2001) and is thought to have been hydrologically-closed during at least part of the lake's history (Buskirk et al., 2016). Part of the formation is protected as the 24.3 km^2 Florissant Fossil Beds National Monument (FLFO), which was established in 1969 primarily to safeguard its paleontological resources. This site preserves compressions/impressions of plant structures, various palynomorphs, diatoms, petrified wood including large *Sequoioxylon pearsallii* (redwood) stumps, invertebrates including one of the most diverse fossilized insect assemblages in the world, and vertebrates such as fish, mammals, and rare birds (Gregory-Wodzicki, 2001; Meyer, 2003; Veatch and Meyer, 2008).

Paleoecological and paleoclimatic reconstructions of the Florissant flora are significant because the flora immediately precedes the Eocene-Oligocene climatic transition (Evanoff et al., 2001; Prothero, 2008). The Florissant Formation is radiometrically dated using $^{40}Ar/^{39}Ar$ of sanidine at the latest Eocene (34.07 ± 0.10 Ma; Evanoff et al. 2001; Fig. 2); corroborating biostratigraphic evidence, i.e., the occurrence of Merycoidodontidae, bronthothere tooth fragments (e.g., *Megacerops* sp.) in the middle shale units, and *Mesohippus* in the lower mudstone unit, indicate a Chadronian age (Evanoff et al., 2001; Lloyd et al., 2008; MacGinitie, 1953; Wood et al., 1941). The radiometric date of 34.07 ± 0.10 Ma (Evanoff et al. 2001) should be considered a minimum age for the plant fossils as they are stratigraphically older than the

units that were dated (Fig. 2). This provides further evidence that these plant macrofossils can be confidently considered latest Eocene. Plant macrofossils of the Florissant Formation were previously revised and documented by MacGinitie (1953), which was interpreted to represent a rich mesic riparian component of temperate and thermophilic elements (e.g., members of Sapindaceae, Anacardiaceae, Juglandaceae, Fabaceae) and an upland component of xeric, chaparral type vegetation that occupied drier hillsides surrounding the paleolake (e.g., evergreen oaks). Plant taxa reported include two genera in the class Polypodiopsida (*Dryopteris* and *Equisetum*), nine species of conifers including members of *Sequoia, Chamaecyparis*, *Picea, Torreya,* and *Pinus*, and ~129 species of angiosperms (MacGinitie, 1953). The most common angiosperms are the extinct taxa *Fagopsis longifolia* (Fagaceae) and *Cedrelospermum lineatum* (Ulmaceae, Manchester, 1989, 2001; Manchester and Crane, 1983). Revisions to MacGinitie (1953) have been made with more recent and stringent taxonomic work (e.g., Manchester, 2001), but still document a similar taxonomic composition and diversity. Additional taxa are known from the fossil pollen record (Bouchal et al., 2016; Leopold and Clay-Poole, 2001; Wingate and Nichols, 2001).

Many prior assessments of the ecology of the Florissant flora, including leaf life span, relied on nearest living relative (NLR) techniques. For example, the taxonomic character of the Florissant flora has similarities to modern seasonally-dry sclerophyllous forests (Bouchal et al., 2014; MacGinitie, 1953) and several plant species were assumed to be evergreen because of the leaf life span of the NLRs. MacGinitie (1953) also argued that the Florissant fossil plants were sourced from both riparian and non-riparian environments by considering the growth habitats of the fossil's NLRs. However, the application of taxon-free approaches, such as leaf mass per area (M_A, Royer et al., 2007, see methods below for more details), to Florissant may provide a more

reasonable reconstruction of the paleoecology of the flora because of the assumptions, potential biases, and shortcomings of paleoecological reconstructions made using NLR techniques (e.g., the dependency on accurate taxonomic identification, the assumption of unchanged ecological tolerances over time, and the poorly known correlation between leaf economic traits and phylogeny whereby unrelated plants may display convergent evolution of morphological traits adaptive to similar environments; see Peppe et al., 2018 for further discussion).

Paleoclimatic estimates, utilizing Florissant's macrofossil and palynology fossil records, have been made using several leaf physiognomic-based and taxon-based methods. Leaf physiognomic methods that have been employed include univariate (e.g., leaf margin analysis [LMA], leaf area analysis [LAA]) and multivariate (Climate Leaf Analysis Multivariate Program [CLAMP]) approaches (e.g., Wilf, 1997; Wilf et al., 1998; Wolfe, 1993) and are advantageous when assessing the Florissant megaflora because they avoid the difficulty of assigning taxonomic affinity to fossils. Taxon-based methods, such as the coexistence approach, non-metric multidimensional scaling of higher taxa, and the bioclimatic approach (e.g., Greenwood et al., 2005; Mosbrugger and Utescher, 1997; Reichgelt et al., 2013; Uhl, 2006) rely on fossils being correctly identified, for climatic tolerances to have remained relatively unchanged, and for the underlying NLR datasets to be robust and representative, which is often not the case (e.g., Grimm et al., 2016; Grimm and Denk, 2012; Grimm and Potts, 2016). Such methods are advantageous at Florissant because they can be applied to any plant organ or taxonomic group—including conifers, which are common at Florissant—rather than just leaves of woody non-monocotyledonous (i.e., "dicotyledonous") angiosperms and some have argued that many leaf traits are strongly correlated with and confounded by phylogeny (Little et al., 2010). However, one of the problems with using taxon-based methods on the Florissant flora is the potential to

incorporate pollen from a large area, including possible lower elevation sites, which may bias paleoclimatic reconstructions (e.g., Baumgartner and Meyer, 2014). At Florissant, taxon-based methods tend to produce higher mean annual temperature (MAT) estimates, ranging widely from 10.0–18.3 °C (Baumgartner and Meyer, 2014; Boyle et al., 2008; MacGinitie, 1953; Zaborac-Reed and Leopold, 2016). In contrast, using the leaf physiognomic proxy CLAMP, Gregory (1994) estimated a MAT of 10.7 ± 1.5 °C and a growing season precipitation of 556 ± 125 $mm \cdot yr^{-1}$. Paleoclimatic estimates using additional paleobotanical proxies, such as Digital Leaf Physiognomy (DiLP) may help clarify ancient climate amidst such widely varying results. Though currently, studies using DiLP are few (e.g., Flynn and Peppe, 2019; Lowe et al., 2018), and further applications of the proxy on fossil floras are required to assess its applicability.

In this study, we carried out a M_A and DiLP analysis on a census collection of fossil leaves from the Florissant Formation to 1) contribute taxon-free paleoecological perspectives on the Florissant flora; 2) provide a case study to further test the applicability of DiLP as a paleoclimatic proxy; and 3) help elucidate the ancient climate in which the Florissant flora existed. In addition, we combine our data with those from previous studies to test for the presence of a 'wet site bias' in tooth-related DiLP variables, and to examine the relationship between M_A and insect leaf herbivory. These analyses provide important information for assessing the climate and ecology across the Eocene-Oligocene transition in the western interior of North America.

2. Material and Methods

2.1. Material

Fossil leaves that had been collected in 2009 and 2010 at Collection Site 9 (38° 55’ N, 105° 17’ W; precise coordinates are available by contacting FLFO paleontology staff) within Florissant Fossil Beds National Monument were examined. A total of 2,300 leaf specimens were collected from Collection Site 9; these are housed in the FLFO collections (Accession Numbers: 422, 450, and 476). A census collection technique was used whereby all plant materials preserved well enough for recognition to morphotype were collected and curated (e.g., Chaney, 1924). The collections were made from a ~5 m stratigraphic section within the middle shale unit of the Florissant Formation, which is dominated by mudstones, siltstones, and finely laminated shales with several interbedded lapilli tuffs indicating that volcanic events occurred with some frequency (Fig. 2). A subset of the fossil leaves from the 2009-10 collection (167 specimens) were used in this study. To build this subset, we scanned the entire collection and included all specimens that could be divided into a unique morphotype, or “a species-like entity,” by considering variation in morphological characters outlined in the *Manual of Leaf Architecture* (Ellis et al., 2009). Morphotypes were numbered randomly to facilitate study; in a few cases the numbers are not continuous because morphotype groups changed after more detailed examination. Specimens representing a morphotype provided leaf margin data at the very least. Additional specimens of a morphotype were only included if they were preserved well enough for DiLP and/or leaf mass per area analyses (see below). Thus, we were unable to reliably calculate morphotype relative abundance. Several leaves were assigned a taxonomic affinity consistent with previously described taxa at Florissant (e.g., MacGinitie, 1953). No new affinities (i.e., previously undocumented taxa from Florissant) were assigned, though several previously undescribed morphotypes were recognized (Fig. 3, Supp. A; Allen et al., 2018).

Fossil leaves were photographed using a Nikon D7000 camera and digitally prepared for M_A and DiLP analysis using Adobe Photoshop™. Whenever possible, multiple leaves per morphotype were analyzed. Foliar characters were measured using the open source software ImageJ (Table S1; http://rsbweb.nih.gov/ij/; Schneider et al., 2012).

2.2. Leaf mass per area reconstructions

Leaf mass per area (M_A) analysis permits the reconstruction of aspects of paleoecology using a taxon-free approach. M_A values have been shown to vary over a leaf economic spectrum, whereby plants adapted to fast-returns (e.g., deciduous plants) invest less in their leaves, resulting in lower M_A values and shorter leaf lifespans, with the opposite true for plants with slow-returns (e.g., evergreen plants; Royer et al., 2010; Royer et al., 2007; Wright et al., 2005). For example, a meta-analysis by Poorter et al. (2009), found the median M_A of deciduous shrubs and trees to be 73 and 75 $g \cdot m^{-2}$ respectively, whereas it was 161 and 106 $g \cdot m^{-2}$ for evergreen shrubs and trees. M_A has also been correlated to various other ecological traits including resistance to foliar herbivores and thus the extent of insect damage on a particular leaf (Poorter et al., 2009; Royer et al., 2010; Royer et al., 2007). Taxa with high M_A tend to have lower rates of insect damage due to tougher and/or thicker leaves (Royer et al., 2007; Wilf et al., 2001); however, the opposite trend has been observed at some sites (e.g., Wappler et al., 2012). Additionally, the distribution of M_A values has been shown to vary between different environments; for example, distributions are centered at lower values in disturbed riparian environments and have wider variance in ever-wet tropical environments (Peppe et al., 2018; Royer et al., 2010).

Leaf mass per area was reconstructed following the protocol of Royer et al. (2007). A brief summary follows: Measurements were only made on leaves (leaflets treated as leaves) with an intact base and/or attached petiole and where it was possible to reconstruct leaf area (Fig. S1). For leaves with an intact petiolar attachment, the petiole width measurement was made by drawing a perpendicular line across the petiole at the location where the basal leaf tissue intersected the petiole (Fig. S1A). When the leaf base was asymmetrical, the measurement was made by drawing a perpendicular line across the petiole at the uppermost contact between the laminar tissue and petiole to the opposite edge of the midvein (Fig S1B). In cases where the leaf had a complete base, but no petiolar attachment, the perpendicular line was drawn across the base of the midvein at the location where the basal leaf tissue came into contact with the midvein (Fig S1C). This location on the leaf is the same as the location of the petiole width measurement made when a leaf has an intact petiole, and thus is measuring the same dimension. When the entire leaf was preserved, leaf area was reconstructed by directly measuring the area of the leaf in ImageJ. In cases where the leaf had minimal damage but its area could be reliably inferred, we reconstructed the damaged portion of the margin. If only a marginal half of the leaf was preserved and we knew or could reliably assume the leaf was medially symmetric (e.g., not a leaflet), leaf area was reconstructed by doubling the area of that half. The petiole width and leaf areas for leaves used to reconstruct M_A are given in the "petiole width" and "inferred blade area" columns in Table S1. When morphotypes were represented by multiple measured specimens, morphotype averages were calculated. In our analyses, we considered M_A results for morphotypes represented by at least two measurable specimens ($N > 1$) and for all morphotypes represented by at least one measurable specimen ($N \geq 1$).

197 *2.3. Digital Leaf Physiognomy*

198 Digital Leaf Physiognomy (DiLP) is a multivariate leaf physiognomic-based proxy that
199 examines continuous foliar characters (e.g., leaf area, tooth size, tooth frequency) which directly
200 and robustly relate to mean annual temperature (MAT) and mean annual precipitation (MAP),
201 rather than the categorical characters used in CLAMP (Huff et al., 2003; Peppe et al., 2011;
202 Royer et al., 2005). DiLP has also been shown to be less sensitive to the 'wet site bias,' whereby
203 riparian zones tend to have more toothed plant species relative to the surrounding forest, and
204 plant fossils are typically sourced from such environments (Kowalski and Dilcher, 2003). Peppe
205 et al. (2011) showed that DiLP estimates on several fossil floras tended to better align with
206 independent paleoclimatic proxy evidence than univariate approaches.

207 Several foliar characters were digitally measured for DiLP analysis following the
208 protocols outlined in Royer et al. (2005) and Peppe et al. (2011). The following is a brief
209 summary of these methods, including digital preparation and measurement phases. First, the leaf
210 (leaflets treated as leaves) was digitally extracted from the matrix and the petiole was separated.
211 If the leaf margin was minimally damaged and either a marginal half of the leaf's area or the
212 entire leaf area could be reliably inferred, the leaf was "repaired" by reconstructing the damaged
213 margin. Second, damaged portions of the margin of toothed leaves, including portions
214 reconstructed for leaf area measurements, were digitally removed. To do so, a selection was
215 made with two lines that were drawn perpendicular to the midvein from where damage on the
216 margin began and ended, and by connecting those two lines along the midvein (Fig. S2B, S2C).
217 If damage started or ended on an incompletely preserved tooth, those lines were drawn from the
218 nearest undamaged sinus as to not include that partial tooth in subsequent internal blade area
219 measurements (see below). Third, a second version of this leaf was created and the teeth were

separated from the leaf blade by making selections between the sinuses of primary teeth (Fig. S2B, S2C).

Measurements on these digitally prepared leaves were then made in ImageJ. First, leaf area and major length was measured on either the entire leaf, or on a marginal half and then doubled ("inferred blade area", "major length", respectively; Fig. S2B). Leaf area included the area of the blade and the petiole when preserved, even if only partially preserved, consistent with the methodology used in the calibration dataset (Peppe et al., 2011; Royer et al., 2005). In cases where the leaf was too incomplete to reliably "repair" at least one marginal half, leaf area was not measured. Second, perimeter and leaf area were measured on the leaf where damaged portions of the margin were removed ("raw perimeter", "raw blade area", respectively; Table S1, Fig. S2B, S2C). Third, the artificial perimeter created by removing damaged portions of the leaf was measured and subtracted from the total leaf perimeter ("total preserved perimeter"; Fig. S2B, S2C). Fourth, perimeter and leaf area were measured on the leaf with teeth removed ("raw internal blade area" and "total preserved internal perimeter"; Fig. S2B, S2C), and the number of teeth were counted. Variables used in the DiLP regressions (e.g., number of teeth per internal perimeter, Feret's diameter ratio, leaf area) were calculated by averaging these measurements within a morphotype, and then averaging morphotype means to produce a site average. The global multivariate regression of Peppe et al. (2011) was used to estimate MAT and MAP. A Northern Hemisphere multivariate regression, which is based on modern calibration sites from North America, Central America, Asia, and Europe, was also used to estimate MAT (Lowe et al., 2018; Peppe et al., 2011).

2.4. Leaf margin and leaf area analyses

Leaf margin analysis (LMA) was also used to estimate MAT using six published univariate regression equations (Kowalski and Dilcher, 2003; Miller et al., 2006; Peppe et al., 2018; Peppe et al., 2011; Wilf, 1997; Wing and Greenwood, 1993; Wolfe, 1979). Standard error for MAT estimates from LMA were calculated using the equation presented in Miller et al. (2006), which accounts for overdispersion in the calibration datasets. Leaf area analysis (LAA) was used to estimate MAP using three published univariate regression equations (Peppe et al., 2018; Peppe et al., 2011; Wilf et al., 1998). Leaf area measurements were made digitally using ImageJ and did not incorporate indirect measurements from leaf size class templates, though the Wilf et al. (1998) regression was originally made using size classes, which may add uncertainty to those measurements (Peppe et al., 2010).

3. Results

3.1. Morphotypes

The late Eocene Florissant flora was taxonomically rich; the subset of fossils analyzed in this study included 66 angiosperm morphotypes (Fig. 3; Supp. A). Of these, 45 are identified taxonomically, whereas an additional 21 are unidentified taxonomically yet are morphologically distinct. The taxonomic composition and relative abundance of our collection was similar to that previously described in other Florissant collections (e.g., MacGinitie, 1953; Manchester, 2001). Taxa represented by five or more specimens include *Fagopsis longifolia*, *Cedrelospermum lineatum*, *Hydrangea fraxinifolia / Staphylea acuminata*, *Vauquelinia coloradensis*, *Caesalpinites acuminatus*, *Quercus* cf. *scottii*, *Rhamnites pseudo-stenophyllus*, *Rhus stellariaefolia*, *Rosa* cf. *hilliae*, *Carya libbeyi*, and *Athyana haydenii*. Thirty-three of the morphotypes were represented by a single specimen.

3.2. Leaf mass per area

Of the 66 angiosperm morphotypes, only 33 were preserved well enough to be included in the M_A analysis. M_A estimates of all measured morphotypes ($N \geq 1$) ranged from 67.7–189.2 $g \cdot m^{-2}$, with an average value of 110.0 $g \cdot m^{-2}$ (Table 1). Nine of the analyzed morphotypes (27%) had M_A values below 87 $g \cdot m^{-2}$, typical for leaves with life spans of less than one year (e.g., deciduous; Royer et al., 2007). Only five morphotypes (15%) had values greater than 129 $g \cdot m^{-2}$, typical for leaves with life spans of more than one year (e.g., evergreen). The majority of morphotypes (58%) had M_A values intermediate of these, suggestive of leaf life spans of around one year (semi-evergreen), though we interpret these as mainly evergreen (Poorter et al., 2009). Estimates from thirteen morphotypes with $N > 1$ ranged from 86–161 $g \cdot m^{-2}$, with an average of 120.2 $g \cdot m^{-2}$, very similar to the average of all measured morphotypes. Estimates of leaf lifespan were also very similar to all measured morphotypes with 8% deciduous, 77% semi-evergreen, and 15% evergreen.

The site averaged value of Florissant is similar to warm Eocene regional lowland sites in Bonanza, Utah and the Bighorn Basin in Wyoming, and is distinct from the sites in the lower Eocene Okanagan Highlands of northern Washington and southern British Columbia (Table 2). The distribution of M_A values is notably different to the comparative modern environments used by other studies (Lowe et al., 2018; Peppe et al., 2018). Instead, it corresponds very well with modern floras collected from non-riparian sites in Californian chaparral and oak-woodland (Fig. 4; see Supp. B for annual climate diagrams of these sites).

We place particular emphasis on the M_A distribution and average of all our measured morphotypes ($N \geq 1$), because it is very similar to the dataset based on specimens with multiple

specimens per morphotype ($N > 1$), and it increases the number of morphotypes used from 13 to 33, which better characterizes the entire floral community. Although we note that in some cases single measured specimens may be outliers relative to a morphotype's average and may lead to erroneous morphotype estimates (e.g., Royer et al., 2007), 71% of Florissant specimens within a morphotype with $N > 1$ produce a M_A estimate that places that specimen within or immediately adjacent to the bin into which their respective morphotype average is placed (Fig. 4), suggesting that there are relatively few outliers in our dataset.

3.3. Paleoclimatic estimates

All 66 morphotypes were included in our DiLP and univariate MAT estimates. Five morphotypes were not sufficiently preserved to use any variables in the DiLP model except margin type. For DiLP MAP estimates, 61 of 66 morphotypes were used; however, 40 morphotypes (60% of the total flora) were preserved well enough to provide data on leaf area, and the remaining 21 only provided data on perimeter ratio and/or the number of teeth per internal perimeter. Thus, only 40 morphotypes were included in the univariate MAP estimates. The number of morphotypes used in both analyses well exceeds the minimum richness recommended for reliable paleoclimatic reconstruction (Burnham et al., 2005).

DiLP estimated MAT using the global regression at 5.5 ± 4 °C (Table 3), only slightly higher than the modern MAT at Florissant (4.1 °C, www.usclimatedata.com). This low temperature estimate is driven predominantly by a low Feret's diameter ratio (FDR), or simply stated, Florissant has a very high proportion of narrow leaves (Fig. 5). Interestingly, the physiognomy of Florissant leaves shares pronounced similarity to leaves of sclerophyllous floras in Tasmania (Fig. 5). The DiLP MAT estimate using the Northern Hemisphere regression is

much warmer, at 11.6 ± 3.3 °C (Table 3). MAT estimates from LMA overlap within uncertainty with the Northern Hemisphere DiLP estimate, ranging from ~10.7–14.0 °C (Table 3).

DiLP estimated a MAP of 740 +608/-334 mm·yr^{-1}, which is nearly double the MAP of Florissant today (428 mm·yr^{-1}, www.usclimatedata.com). The LAA regression of Wilf et al. (1998) produced lower estimates of 539 +233/-163 mm·yr^{-1}, and the LAA regression of Peppe et al. (2011) produced a slightly higher estimates of 978 +822/-447 mm·yr^{-1} (Table 3).

4. Discussion

4.1. Floral Paleoecology

4.1.1. Sclerophylly

Previous work (e.g., Bouchal et al., 2014; MacGinitie, 1953) described the latest Eocene Florissant flora as having a strong representation of taxa typical of sclerophyllous vegetation zones thought to have been mainly occupying the drier hillsides around ancient Lake Florissant (e.g., *Quercus, Cercocarpus, Vauquelinia*), while more water-dependent riparian taxa grew close to the lake's edge (e.g., *Sequoia, Fagopsis longifolia, Cedrelospermum lineatum, Salix, Populus*). Our study provides taxon-free evidence that supports these earlier interpretations of Florissant by strongly suggesting that the paleoecology of the late Eocene Florissant flora shares physiognomic similarities (e.g., leaf mass per area (M_A) distributions, low Feret's diameter ratio, and low leaf area; Figs. 4 and 5) with modern seasonally dry sclerophyllous vegetation zones.

The distribution of M_A values has been shown to vary between environmental and climatic regimes, and previous studies have demonstrated that M_A distribution in fossil floras reflects these modern distributions in expected ways (Flynn and Peppe, 2019; Lowe et al., 2018;

Peppe et al., 2018; Royer et al., 2010). The distribution of Florissant M_A values is centered at higher values relative to various wet temperate sites and is lacking leaves with the extremely high M_A values found in typical wet tropical sites (Fig. 4). This suggests that the Florissant flora contained more plants employing strategies on the slow-return/high-investment end of the economic spectrum than characteristic wet temperate distributions, and agrees with a predominance of sclerophyllous leaves, which require high investments and are typically long-lived (Chabot and Hicks, 1982). Florissant's distribution also lacks a high proportion of morphotypes with very low M_A values in the 20–60 $g \cdot m^{-2}$ range, which are common in riparian and seasonally dry tropical sites (Fig. 4). For example, numerous taxa with M_A values in that range were found to characterize a summer-wet tropical forest in Panama influenced by drought deciduousness (Fig. 4E, Reich, 1995). In contrast, many modern chaparral floras lack an important element of drought deciduous taxa and are instead dominated by evergreen taxa (Keeley, 1999). Florissant's sclerophyllous-like physiognomy is also highlighted by the close correspondence in M_A distribution to a chaparral site in Half Moon Bay, California (Fig. 4).

When compared to the global regression of Peppe et al. (2011), Florissant has a low site-mean Feret's diameter ratio (FDR; 0.514), owing to a high abundance of narrow leaves (Fig. 5). High length to width ratios in leaf litter from modern Australian forests were characteristic of seasonally dry sclerophyllous forests, much more so than other Australian vegetation types (Greenwood, 1996). Leaves with high length to width ratios enhance sensible heat loss during summer droughts, minimizing leaf death from overheating (Yates et al., 2010). Further, such low FDR values are even rarer in the calibration dataset for leaves with mid-range number of teeth per internal perimeter values, which is a characteristic of the Florissant fossil flora (~1.5–3; Fig.

5). Two sites in Tasmania share this physiognomic feature most closely with Florissant, a wet-sclerophyllous forest and a wet heathland/scrub (Fig. 5; Supp. B).

Woody evergreen plants in Mediterranean-type climates (i.e., dry summers, wet mild winters) are very commonly characterized by sclerophyllous leaves with low leaf area; an adaptation for hot dry summers (Ackerly et al., 2002; Mooney and Dunn, 1970). Fossil leaf sizes at Florissant are small, with all but one measured morphotype in this collection being microphyll in size. The leaf size index (LSI = (%microphyll or smaller + 2·%nanophyll + 3·%mesophyll or larger)/2) is 1.25 and the average leaf area is 356 mm^2 (n = 40 morphotypes; average of morphotype averages). The leaf size estimates are much smaller than that observed in a study of modern leaf litter samples in Australia (LSI=13–59, excluding a microphyll fern forest; Greenwood, 1994), and smaller than Laguna del Hunco (LSI=31), an early Eocene Patagonian fossil plant site thought analogous to modern Australian forests (Merkhofer et al., 2015). In the DiLP calibration dataset, modern sites with leaf areas of $\leq$ 500 mm^2 include heathland/scrub vegetation and forests in Australia (Frodsham, Tasmania) and New Zealand (Kaimanawa Mountains, Gouland Downs, and Foxton Estuary) and desert floras of Mexico (Empalme and Cabo San Lucas). Most chaparral species have leaf sizes ranging from 100–500 mm^2 (Keeley, 1999) and in a sample of 22 naturally growing chaparral species, the average leaf size was 1240 mm^2 (median = 405 mm^2), with 59% of species having leaves <550 mm^2 (Ackerly et al., 2002). In equatorial Africa, microphyll leaves are dominant in seasonally-dry woodlands, whereas both mesophyll and microphyll leaves are common in forests that do not experience a pronounced dry season (Jacobs, 2004). It is possible that the sampled fossil flora at Florissant underestimates leaf area due to taphonomic exclusion of large leaves (e.g., Burnham, 1989; Greenwood, 1992; Roth and Dilcher, 1978). However, Hagen et al. (2019) found that leaf fragmentation of large leaves

during fluvial transport and fossil excavation, which would cause the exclusion of those fragmented leaves from leaf area analyses, did not result in significant underrepresentation of large leaves. Importantly, the taphonomic bias against large leaves is expected to be greater in the transported channel assemblages assessed by Hagen et al. (2019), compared to the lacustrine assemblage of Florissant. In addition, the close similarity of average leaf size in our Florissant collection to modern sclerophyllous vegetation zones is in agreement with the other physiognomic features discussed above, suggesting that sclerophyllous vegetation was an important component of the Florissant flora.

Although it appears sclerophylly was an important component of the Florissant flora, it is important to note that both the local and regional vegetation was spatially heterogenous, which is best highlighted by the presence of redwood fossils at Florissant, including stumps up to 15 m in circumference (Gregory-Wodzicki, 2001). For example, Bouchal et al. (2014) found some modern relatives of Florissant's taxa to be important members of the "laurel forest zone," which occurs in perhumid climates (MAP ≈ 1000–2000 $mm \cdot yr^{-1}$) with mild winters (Körner, 2013). This zone is characterized by laurophyllous leaves which share some physiognomic similarity to sclerophyllous leaves (e.g., elongate with thick cuticles), but are often untoothed. Sclerophyllous vegetation zones (MAP ≈ 400–1100 $mm \cdot yr^{-1}$) often border and even grade into more mesic laurophyllous forests, such as in eastern Australia, Tasmania, and Chile (Axelrod, 1975; Körner, 2013). Axelrod (1975) proposed that sclerophyllous vegetation evolved from laurophyllous vegetation that was globally dominant in the Eocene as global climates dried through the late Paleogene and Neogene. The majority of Florissant leaves analyzed in this study were small, toothed, had no additional features such as drip tips that would suggest local perhumid conditions, and are thus interpreted as mainly sclerophyllous, rather than laurophyllous, leaves.

As Boyle et al. (2008) highlights, there does not seem to be a single modern analog to Florissant and the vegetation heterogeneity documented at Florissant was very likely influenced by the topographically diverse upland landscape in which this ancient flora lived (Meyer, 2001).

4.1.2. Physiognomy of riparian taxa: 'the wet site bias'

Bouchal et al. (2014) ascribed Florissant taxa to four major vegetation types using NLR inference: sclerophyllous, nemoral coniferous forest, mesic broad-leaved forest, and riparian. Here we utilize this work and combine those vegetation type inferences with physiognomic data from the same species (excluding questionable taxonomic assignments), to test for a 'wet site bias.' The 'wet site bias' concept is the observation that there is a greater concentration of toothed-leaved taxa growing near the water's edge relative to the surrounding vegetation, possibly due to riparian characteristics such as greater water availability, habitat openness, and more frequent disturbance (Burnham et al., 2001; Greenwood et al., 2005; Kowalski and Dilcher, 2003). We assess whether this bias extends to the continuous tooth characters measured using the DiLP protocol, including perimeter ratio (i.e., ratio of internal to external perimeter) and the number of teeth per internal perimeter.

Of the Florissant taxa ascribed to the riparian zone (Bouchal et al., 2014) and with reliable taxonomic correspondence to our specimens, 91% have toothed leaves, compared to 58% of taxa ascribed to non-riparian types, which are assumed to be growing some distance to the shore. There are significant differences in both the perimeter ratio and the number of teeth per internal perimeter between the two vegetation types (Fig. 6; Table S2). Such a pronounced difference suggests that late Eocene riparian environments may have concentrated species having leaves with many and larger teeth, in addition to, simply leaves with teeth present. This is

consistent with a similar observation by Peppe et al. (2011), and whereas such differences are apparent, their impact on DiLP generated MAT reconstructions appear to be minimal (Peppe et al., 2011).

4.1.3. Leaf herbivory and economics

We examined the leaf mass per area estimates from our analysis in conjunction with the insect damage data of Smith (2000, 2008) to test for a correspondence (i.e., more damage on taxa with lower M_A values). We limited this to morphotypes in our analysis that had both a M_A value and a taxonomic identification that could be confidently matched to Smith's (2000, 2008) data. Smith (2000, 2008) examined more than 600 non-monocotyledonous angiosperm leaves from the middle shale (localities 5 and 7) of the Florissant Formation for insect damage. Overall, 22% of the identifiable genera from Florissant lacked evidence of insect damage (Smith, 2008). Smith (2008) notes that the four most abundant genera in her sample (C*edrelospermum, Fagopsis, Staphylea,* and *Rhus*) account for 50% of the leaves and 44% of the damage.

There is no significant relationship between our leaf mass per area (M_A) data and either percent of leaves damaged (n = 15, p = 0.277, r^2 = 0.09) or percent of area damaged (n = 15, p = 0.416, r^2 = 0.05). However, there is some evidence to suggest that leaves in the Florissant flora follow predicted patterns of low insect damage and high M_A and vice versa (e.g., Poorter et al., 2009). Leaves of *Fagopsis longifolia* are abundant and easy to recognize in the Florissant flora. Smith (2000, 2008) had 123 leaves of *Fagopsis longifolia* in her sample, of which only 4% had insect damage with none classified as specialized damage. Our M_A value for *Fagopsis longifolia* (n = 7) averaged to 104.2 $g \cdot m^{-2}$, suggesting a leaf lifespan of approximately one year. A similar pattern is observed in *Cedrelospermum lineatum.* This species is also represented by a large

sample size (n = 127 leaves) in Smith's (2008) dataset, but only 26.8% were damaged. Whereas specialized damage is found on leaves of *C. lineatum*, only ~1% of the total leaf area was eaten or damaged (Smith, 2008). Our leaf mass per area results for *Cedrelospermum lineatum* also indicate a leaf lifespan of approximately one year (126.1 $g \cdot m^{-2}$; n = 5).

Smith (2008) reviewed 10 leaves of *Rhamnites pseudo-stenophyllus*, none of which had damage. This taxon (n = 4) has a leaf mass per area estimate of 161.0 $g \cdot m^{-2}$, suggesting an evergreen habit. Only one of the eight leaves of *Vauquelinia* examined by Smith (2008) had damage, and this accounted for less than 1% of the total leaf area. The estimated leaf mass per area was 137.5 $g \cdot m^{-2}$ (n = 6) with a leaf lifespan of greater than one year (evergreen). *Staphylea acuminata/Hydrangea fraxinifolia* showed correspondence in the opposite pattern. Smith (2008) did not have any data for *Hydrangea fraxinifolia*, but in our analysis, *S. acuminata* and *H. fraxinifolia* were considered as indistinguishable morphotypes and therefore were combined. As predicted, we found this morphotype (combined *Staphylea* and *Hydrangea*) had a low leaf mass per area of 86.0 $g \cdot m^{-2}$ (n = 6) with a leaf lifespan of less than one year. It had a high amount of damage (68% of leaves were damaged by insects, which accounted for 3.9% of the total leaf area), which included observations of specialized damage (Smith, 2008). Taken together, although there was no significant correlation between M_A and insect damage, these qualitative results indicate that several leaves with short leaf lifespan (e.g., *Staphylea* and *Hydrangea*) were more heavily damaged than taxa with leaf lifespans of $\geq$ 1 year (e.g., *F. longifolia, C. lineatum, R. pseudo-stenophyllus*, and *Vauquelinia*). Long-lived leaves at Florissant were apparently not particularly palatable to insects, possibly caused by low nitrogen content as suggested by high leaf mass per area values, or due the presence of anti-herbivory defense compounds (Poorter et al., 2009).

It is possible that the high percentage of sclerophyllous taxa at Florissant contributed to the generally low rates of insect herbivory. Turner (1994) comments that the primary function of sclerophyllous leaves is protection. It is challenging for an insect to insert their mouthparts in the stronger and tougher leaves that characterize sclerophyllous vegetation (Turner, 1994). For example, the early to middle Eocene Green River flora has higher rates of herbivory and likely a lower percentage of sclerophyllous taxa than Florissant (Smith, 2008). MacGinitie (1969) divided the Green River flora into four vegetation groups. He noted that the vegetation regime (group 2) that was of "higher ground" up to about 610 m above the lake surface elevation in lower water table areas was likely sclerophyllous. This group of 18 genera includes some that are also recognized as sclerophyllous at Florissant (e.g., *Quercus* and *Vauquelinia*). However, there were significantly more taxa, especially those bordering the lake or in areas with a high water table, that would have been quite palatable (i.e., not sclerophyllous) to insects in the Green River flora. Smith (2008) hypothesized that the decreased rates of herbivory between the early to middle Eocene Green River flora and the late Eocene Florissant flora may have been due to the higher paleoelevation at Florissant or the cooler global temperatures later in the Eocene. Yet, some floras of similar age and elevation to Green River (e.g., Blue Rim [~49 Ma, southwestern Wyoming]; Allen, unpublished data) have extremely low rates of herbivory. There is probably no one factor that contributed to the differences in herbivory between the Green River and Florissant floras (Smith, 2008), though differences in the proportion of sclerophyllous taxa and/or evergreen taxa plausibly explain some of the differences.

4.2. A comparison of paleobotanical methods for climate reconstruction

493 Leaf physiognomic models are based on the general principles that a higher proportion of
494 toothed leaves of woody non-monocotyledonous angiosperms in a flora indicate a colder MAT
495 and larger mean leaf size indicate a higher MAP (see review in Peppe et al., 2018). Mean annual
496 temperature and MAP estimates made using leaf physiognomic models are in general agreement
497 for Florissant (Table 3 and 4). Precipitation estimates using DiLP and LAA overlapped within
498 uncertainty (Table 3). All estimates indicate that Florissant was relatively dry with a MAP <1000
499 $mm \cdot yr^{-1}$ (Table 3, Körner, 2013).

500 Leaf Margin Analysis (LMA), which uses the presence or absence of teeth along the leaf
501 margin to estimate temperature (Wilf, 1997), consistently estimated a MAT for Florissant of 11–
502 12 °C (Table 3), with the exception of the Kowalski and Dilcher (2003) model, which estimated
503 MAT as 14.3 ± 3.6 °C. The Kowalski and Dilcher (2003) model is based on the principle that
504 there are more toothed taxa in riparian environments and that riparian environments are more
505 likely to preserve fossil leaves (e.g., Burnham et al., 2001), which could lead to an
506 underestimation of MAT if modern calibrations are biased against 'wet' sites. However, the
507 extent to which this 'wet site bias' adds inaccuracy or uncertainty to MAP estimates is not well
508 known (Peppe et al., 2011), and the limited number of modern sites used in the Kowalski and
509 Dilcher (2003) model may result in an overestimation of MAT. It should also be noted that LMA
510 is hypothesized to be more robust in a mesic flora rather than a seasonally dry flora (Wolfe,
511 1993). Thus, as Florissant was likely a seasonally dry flora, the error bars on our LMA analyses
512 should be considered minima.

513 CLAMP is a multivariate model that uses 31 discrete characters (e.g., presence of teeth,
514 apex and base shape, length to width ratio) to estimate 11 climate parameters including MAT
515 (Spicer et al., 2009; Wolfe, 1993; Wolfe and Spicer, 1999). CLAMP has been applied to the

Florissant leaf collections and has produced MAT results ranging from 10–14 °C (Table 4, Gregory-Wodzicki, 2001; Gregory, 1994; Gregory and Mcintosh, 1996; Wolfe, 1992; Wolfe et al., 1998). Digital leaf physiognomy is a multivariate model that uses continuous variables to reconstruct MAT and MAP (Peppe et al., 2011; Royer et al., 2005). The MAT DiLP estimates for Florissant, using either the global regression or the Northern Hemisphere regression, overlap within uncertainty with most other MAT estimates (Table 3, Table 4). However, given the occurrence of thermophilic taxa present in the ancient flora, including *Vauquelinia* and a palm (Leopold and Clay-Poole, 2001; Manchester, 2001; Zaborac-Reed and Leopold, 2016), MAT estimates using the DiLP global calibration are unusually cold. Thus, we favor the estimates made using the Northern Hemisphere regression.

Mean annual temperature estimates for Florissant using taxonomic information (i.e., NLR estimates) are generally warmer (e.g., 14–18 °C; Table 4) than those using leaf physiognomy (e.g., 11–14 °C; Table 3, Table 4). This pattern is consistent with other fossil floras where multiple methods have been applied including the early Eocene Republic site in Washington, USA (Greenwood et al., 2005; Wolfe, 1994; Wolfe et al., 1998). At Florissant, the warmer estimates from nearest-living relative approaches are potentially the result of including pollen taxa that are sourced from sites from lower elevations that were warmer (e.g., Baumgartner and Meyer, 2014). Furthermore, there are biases in various taxonomic databases (e.g., the Paleoflora database), sources of climate data, and confidence in taxonomic assignments (e.g., Grimm et al., 2016; Grimm and Denk, 2012; Grimm and Potts, 2016). In some analyses (e.g., Baumgartner and Meyer, 2014), the “warmest” taxa in the literature for Florissant are also the most contentious in terms of an accurate identification; when these are removed to create a list with more confidently identified taxa, temperature estimates were colder. Based on this, we interpret the MAT

estimates made using leaf physiognomy to generally be a more accurate estimate for the climate of the Florissant flora.

All of the leaf physiognomic estimates (univariate and multivariate) for MAT and MAP overlap within uncertainty, and the uncertainty associated with the univariate estimates of MAT is generally lower than the DiLP estimates (Table 3). This suggests that the extra processing time required to apply to DiLP to a fossil flora may not provide much additional information or increase the accuracy of the estimates. However, as discussed by several authors (e.g., Peppe et al., 2018; Royer et al., 2012), the uncertainty associated with estimates made using leaf margin analysis are the minimum uncertainty and are likely underestimates. As an example, other than the Peppe et al. (2011) and Peppe et al. (2018) univariate models, the calibration datasets for the leaf margin analysis univariate models are relatively small (<40 floras), which does not capture the true variability in the relationship between leaf margin and MAT.

Furthermore, whereas the DiLP estimates overlap within uncertainty with the univariate methods, we were able to use information from several of the DiLP variables to better constrain the paleoclimate and paleoecology of the Florissant flora, which would not have been possible if we had only used the univariate methods. For example, the low MAT estimate (5.5 ± 4 °C) using the global regression of DiLP (Peppe et al., 2011) in this study is driven by the site's combination of low FDR and relatively moderate number teeth per internal perimeter, which are most similar to a wet-sclerophyllous forest and a heathland/scrub in Tasmania (Fig. 5). In general, this combination of linear-shaped leaves with abundant teeth relative to the internal perimeter are rare in the modern global regression (Peppe et al., 2011), which results in an anomalously cold estimate of MAT when the global regression is used. As discussed above, this pattern at Florissant is probably because the fossil flora was sclerophyllous, and sclerophyllous

floras are undersampled in the DiLP calibration dataset. Estimates made for Florissant using the Northern Hemisphere regression are warmer (11.6 ± 3.3 °C vs. 5.5 ± 4 °C), primarily because the Northern Hemisphere regression does not incorporate FDR. Thus, the additional information provided by the DiLP variables considerably enhanced our interpretation of the paleoecology and paleoclimate of the flora. However, the anomalously cold estimate that was made using the global DiLP regression also suggests that caution is needed when applying DiLP to a flora for which there are few or no close modern analogs in the calibration dataset.

Taken together, our results suggest that the DiLP climate estimates provided similar paleoclimate estimates to the univariate methods for the Florissant flora, but also provided important additional information that was crucial to our interpretations about the paleoecology and potential climate regime of the flora. Though considerably more time consuming, the DiLP estimates and DiLP leaf trait variables offered important insights into the flora that would not otherwise have been available. Thus, we suggest that DiLP is a useful tool that can be applied to fossil floras to provide both quantitative reconstructions of paleoclimate and more wholistic, quantitative and qualitative assessments of the paleoclimate and paleoecology of fossil floras.

4.3. Florissant's latest Eocene climate

The Florissant flora records climatic conditions occurring just before the Eocene-Oligocene (E-O) boundary, providing critical insight into the response of plant communities to changing continental climates across the E-O in the western interior of North America (e.g., Meyer, 2016). Leaf physiognomic estimates of climate using leaves from Florissant demonstrate that regional climates were cool (MAT ≈ 12 °C, range for all estimates including uncertainty = 6.5 – 17.9 °C) and dry (MAP ≈ 630 mm·yr^{-1}, range for all estimates including uncertainty = 287

– 1564 mm·yr^{-1}) relative to early and middle Eocene western North American sites (see below; Table 3 and 4). Low leaf sizes, low Feret's diameter ratio, and the distribution of leaf mass per area of Florissant leaves also suggests that rainfall was distributed seasonally. A seasonally dry climate agrees with prior ecological interpretations from pollen and macrofossils, suggesting that the dry hillsides existing beyond the riparian zone represented an open, low biomass, woody savanna (Bouchal et al., 2014; Leopold et al., 1992; MacGinitie, 1953). Despite much of the Northern Hemisphere mid-latitudes being covered in warm temperate vegetation in the late Eocene, several older upland localities in the western United States contain considerable sclerophyllous components in their flora including Thunder Mountain in central Idaho, and Little Mountain (southwestern Wyoming) and Green River (northwestern Colorado and northeastern Utah; Utescher and Mosbrugger, 2007).

The close correspondence of Florissant's physiognomic features to floras in winter-wet Mediterranean-type climates, including California chaparral and oak woodland, and sclerophyllous forests in south Australia (Figs. 4 and 5), lends support to a winter-wet inference, contrasting with previous NLR inferences. Mesic elements may have persisted in the riparian zone through summer drought by accessing available ground water near the lake's edge. Although MacGinitie (1953) described "chaparral type" vegetation at Florissant, he inferred a summer-wet precipitation regime by relating Florissant to modern floristic analogs in summer-wet climates of western Texas and northeastern Mexico. However, many of the NLRs of Florissant sclerophyllous vegetation are represented in both summer-wet and winter-wet regimes (Bouchal et al., 2014). Gregory-Wodzicki (2001) found high mean ring width in Florissant *Sequoioxylon* wood, relative to modern *Sequoia* and *Sequoiadendron* wood, and explained this by the presence of ample water availability during the growing season, inferring a summer-wet

608 regime (see also Gregory, 1994). Huber and Goldner (2012) simulated an Eocene North
609 American monsoon (summer) that extended as far north as 60 °N, though the model both ignores
610 potentially important changes occurring throughout the Eocene and its large grid scale likely
611 oversimplified complex topographic interactions in the Rocky Mountain region. In summary, a
612 seasonal precipitation regime at Florissant is clear (e.g., Gregory, 1994), and whereas
613 physiognomic comparisons of this study suggest a winter-wet regime, such an inference is not
614 yet conclusive.

615 Similar MAT and MAP estimates occur at other late Eocene to early Oligocene Rocky
616 Mountain and western interior sites, indicating a regional trend. This includes the Fossil Basin
617 floras (MAT ≈ 12–14 °C, growing season precipitation ≈ 920–1280 mm·yr-1; Lielke et al., 2012)
618 and Beaverhead Basin floras (MAT ≈ 14–15 °C, growing season precipitation ≈ 550–1170
619 mm·yr-1; Lielke et al., 2012) in southwestern Montana, the Haynes Creek flora in eastern Idaho
620 (~30.7 Ma, MAT ≈ 12.5 °C, MAP ≈ 890 mm·yr-1, Axelrod, 1998), the House Range flora in
621 western Utah (~31.4 Ma, MAT ≈ 13.2 ± 2.9 °C, growing season precipitation ≈ 850 ± 300
622 mm·yr-1, Gregory-Wodzicki, 1997), and the Pitch-Pinnacle flora in Colorado (~32.9 Ma, MAT ≈
623 12.7 ± 3.3 °C, growing season precipitation ≈ 1010 ± 300 mm·yr-1, Gregory-Wodzicki, 1997). In
624 addition, late Eocene paleosols in NE Colorado have characteristics similar to modern grassland
625 soils (Hembree and Hasiotis, 2007), and a late Eocene paleosol in SW Montana has
626 characteristics similar to modern desert shrubland soils (Retallack, 2007). This contrasts with
627 climate estimates from early to middle Eocene floras of the western interior, such as the Green
628 River flora (~53.5-48.5 Ma, MAT ≈ 17-19 °C, MAP ≈ 600-900 mm·yr-1, MacGinitie, 1969;
629 Wilf, 2000; Wolfe, 1994) and the Kisinger Lakes flora (~48.5 Ma, MAT ≈ 15-23 °C, MAP ≈
630 900-1400 mm·yr-1, MacGinitie, 1974; Wolfe, 1994), which are markedly warmer and possibly

wetter. This comparison between early and middle Eocene floras from the western interior of North America with the late Eocene Florissant flora indicates a pronounced shift towards cooler and drier climates into the late Eocene prior to the Eocene to Oligocene boundary (E-O) transition. It should be noted, however, that these paleoclimatic comparisons between middle and late Eocene floras could be complicated by differences in paleoelevation. A pre E-O transition to drier conditions was also recorded by decreased chemical weathering and depth to Bk horizon in paleosols of Nebraska and Oregon, though a similar drying trend was not evident in Montana (Sheldon and Retallack, 2004). In north-central Oregon, leaf physiognomy temperature estimates suggest a 5–9 °C cooling occurred between 43 and 38 Ma, well before the E-O transition (Dillhoff et al., 2009; Manchester, 2000; Smith et al., 1998; Wolfe, 1971, 1972). Phytoliths may also provide evidence of a pre E-O opening of landscapes in the Rocky Mountains, as putative PACMAD grasses that may indicate open habitats were abundant in SW Montana during the late Eocene (Strömberg, 2005). This is in contrast to the Central Plains, which were characterized by closed forests with palms, bamboos, and pooid and PACMAD grasses in the late Eocene, not transitioning to open habitats until the late Oligocene-Miocene (Strömberg, 2005, 2011). Thus, leaf physiognomy data of this study support the inference of a pronounced pre E-O climatic transition to cooler and drier climates in the western interior of North America and provide critical data for future comparison of climate and vegetation across the E-O boundary.

5. Conclusions

Florissant's fossil flora grew and was deposited just before the Eocene-Oligocene boundary, a key transition into the globally cooler second half of the Cenozoic. This work provides additional data to supplement our understanding of the paleoecological and

paleoclimatological conditions at the end of the Eocene. Leaf mass per area demonstrated that the majority of Florissant leaves have a leaf lifespan of greater than or equal to one year. This relatively long leaf life span, coupled with the small size of the leaves in the flora and the relatively low Feret's diameter ratio, provides support for the hypothesis that Florissant was comprised of abundant sclerophyllous vegetation. Interestingly, insect damage rates were also relatively low in abundant and taxonomically recognizable taxa preserved at Florissant with high leaf mass per areas, further supporting the sclerophyllous flora hypothesis. Although DiLP estimated an unusually cool MAT of 5.5 ± 4 °C using the global calibration regression, the Northern Hemisphere DiLP regression estimated MAT to be 11.6 ± 3.3 °C, which was very similar to previously published CLAMP estimates and our LMA estimates. DiLP and LAA mean annual precipitation estimates were all within uncertainty and indicate a relatively dry climate (500–1000 $mm \cdot yr^{-1}$), similar to modern day San Francisco, California (600 $mm \cdot yr^{-1}$; www.usclimatedata.com)

These paleoclimatic results suggest that the Florissant flora represented a temperate shrubland to forest biome. Taken together, our paleoecological and paleoclimatic reconstructions for Florissant suggest that beyond the riparian forest, a sclerophyllous shrubland or woodland existed, with physiognomic similarities to modern chaparral, in a seasonally dry climate. These findings provide support for a long-term cooling and drying trend in the western interior of North America before the Eocene- Oligocene boundary.

Acknowledgements

This work was initiated while SEA and AJL were being funded by the Geoscientists-in-the-Parks (GIP) program, a collaboration between the National Park Service, the Geological

Society of America, the Stewards Individual Placement Program, and Americorps. The fossil specimens were collected and photographed by previous Florissant Fossil Beds National Monument paleontology staff members and interns. Thank you to Conni O'Connor and Mariah Slovacek at Florissant Fossil Beds National Monument for logistical assistance. The stratigraphic column of Collection Site 9 (Fig. 2C) was modified from an unpublished work of Katie Card. Travel funding and support from Florissant Fossil Beds National Monument is gratefully acknowledged to SEA. Thank you also to Johannes M. Bouchal and two anonymous reviewers whose careful feedback greatly improved the manuscript.

Appendices

Supplement A: Morphotype catalog

Supplement B: Climate diagrams

Figure S1: Protocol for measuring leaf area and petiole width.

Figure S2: Protocol for measuring digital leaf physiognomy variables.

Table S1: DiLP data

Table S2: Riparian vs. Non-riparian vegetation type

References

Ackerly, D.D., Knight, C., Weiss, S., Barton, K., Starmer, K., 2002. Leaf size, specific leaf area and microhabitat distribution of chaparral woody plants: contrasting patterns in species level and community level analyses. Oecologia 130, 449-457.

Allen, S.E., Meyer, H.W., Thornton, C., Manchester, S.R., 2018. Incertae sedis: Unidentified late Eocene plants in the collection of Florissant Fossil Beds National Monument, Botany 2018, Rochester, MN.

Axelrod, D.I., 1975. Evolution and Biogeography of Madrean-Tethyan Sclerophyll Vegetation. Ann. Missouri Bot. Gard. 62, 280-334.

Axelrod, D.I., 1998. The Oligocene Hayne Creek Flora of Eastern Idaho. University of California Press, Berkeley.

Baumgartner, K.A., Meyer, H.W., 2014. Coexistance climate analysis of the late Eocene Florissant flora, Colorado, 2014 GSA Annual Meeting, Vancouver, British Columbia.

Bouchal, J.M., Zetter, R., Denk, T., 2016. Pollen and spores of the uppermost Eocene Florissant Formation, Colorado: a combined light and scanning electron microscopy study. Grana 55, 179-245.

Bouchal, J.M., Zetter, R., Grimsson, F., Denk, T., 2014. Evolutionary trends and ecological differentiation in early Cenozoic Fagaceae of western North America. American Journal of Botany 101, 1332-1349.

Boyle, B., Meyer, H.W., Enquist, B., Salas, S., 2008. Higher taxa as paleoecological and paleoclimatic indicators: A search for the modern analog of the Florissant fossil flora, in: Meyer, H.W., Smith, D.M. (Eds.), Paleontology of the Upper Eocene Florissant Formation, Colorado. Geological Society of America Special Paper 435, pp. 33-51.

Burnham, R.J., 1989. Relationships between standing vegetation and leaf litter in a paratropical forest: Implications for paleobotany. Review of Palaeobotany and Palynology 58, 5-32.

Burnham, R.J., Ellis, B., Johnson, K.R., 2005. Modern Tropical Forest Taphonomy: Does High Biodiversity Affect Paleoclimatic Interpretations? Palaios 20, 439-451.

Burnham, R.J., Pitman, N.C.A., Johnson, K.R., Wilf, P., 2001. Habitat-related error in estimating temperatures from leaf margins in a humid tropical forest. American Journal of Botany 88, 1096-1102.

Buskirk, B.L., Bourgeois, J., Meyer, H.W., Nesbitt, E.A., 2016. Freshwater molluscan fauna from the Florissant Formation, Colorado: paleohydrologic reconstruction of a latest Eocene lake. Can. J. Earth Sci. 53, 630-643.

Chabot, B.F., Hicks, D.J., 1982. The ecology of leaf life spans. Annual Review of Ecology and Systematics 13, 229-259.

Chaney, R.W., 1924. Quantitative studies of the Bridge Creek flora. American Journal of Science 8, 127-144.

Currano, E.D., Labandeira, C.C., Wilf, P., 2010. Fossil insect folivory tracks paleotemperature for six million years. Ecological Monographs 80, 547-567.

733 Dillhoff, R.M., Dillhoff, T.A., Dunn, R.E., Myers, J.A., Strömberg, C.A.E., 2009. Cenozoic
734 paleobotany of the John Day Basin, central Oregon, in: O'Connor, J.E., Dorsey, R.J., Madin, I.
735 (Eds.), Volcanoes to Vineyards: Geologic Field Trips through the Dynamic Landscape of the
736 Pacific Northwest. Geological Society of America, pp. 135-164.

737 Ellis, B., Daly, D.C., Hickey, L.J., Johnson, K.R., Mitchell, J.D., Wilf, P., Wing, S.L., 2009.
738 Manual of Leaf Architecture. Cornell University Press, Ithaca, New York, USA.

739 Evanoff, E., Mcintosh, W.C., Murphey, P.C., 2001. Stratigraphic summary and $^{40}Ar/^{39}Ar$
740 geochronology of the Florissant Formation, Colorado, in: Evanoff, E., Gregory-Wodzicki, K.M.,
741 Johnson, K.R. (Eds.), Fossil flora and stratigraphy of the Florissant Formation, Colorado. Denver
742 Museum of Nature & Science, Denver, pp. 1-16.

743 Flynn, A., Peppe, D.J., 2019. Early Paleocene tropical forest from the Ojo Alamo Sandstone, San
744 Juan Basin, New Mexico, USA. Paleobiology 45, 612-635.

745 Greenwood, D.R., 1992. Taphonomic constraints on foliar physiognomie interpretations of Late
746 Cretaceous and Tertiary palaeoeclimates. Review of Palaeobotany and Palynology 71, 149-190.

747 Greenwood, D.R., 1994. Palaeobotanical evidence for Tertiary climates, in: Hill, R.S. (Ed.),
748 History of the Australian vegetation, Cretaceous to Recent. Cambridge University Press,
749 Cambridge, pp. 44-59.

750 Greenwood, D.R., 1996. Eocene monsoon forests in central Australia? Australian Systematic
751 Botany 9, 95-112.

752 Greenwood, D.R., Archibald, S.B., Mathewes, R.W., Moss, P.T., 2005. Fossil biotas from the
753 Okanagan Highlands, southern British Columbia and northeastern Washington State: climate and
754 ecosystems across an Eocene landscape. Can. J. Earth Sci. 42, 167-185.

755 Gregory-Wodzicki, K.M., 1997. The Late Eocene House Range Flora, Sevier Desert, Utah:
756 Paleoclimate and Paleoelevation. Palaios 12, 552-567.

757 Gregory-Wodzicki, K.M., 2001. Paleoclimate implication of tree-ring growth characteristics of
758 34.1 Ma *Sequoioxylon pearsallii* from Florissant, Colorado, in: Evanoff, E., Gregory-Wodzicki,
759 K.M., Johnson, K.R. (Eds.), Fossil flora and stratigraphy of the Florissant Formation, Colorado.
760 Denver Museum of Nature & Science, Denver, pp. 163-186.

761 Gregory, K.M., 1994. Palaeoclimate and palaeoelevation of the 35 Ma Florissant flora, Front
762 Range, Colorado. Palaeoclimates 1, 23-57.

763 Gregory, K.M., Mcintosh, W.C., 1996. Paleoclimate and paleoelevation of the Oligocene Pitch-
764 Pinnacle flora, Sawatch Range, Colorado. GSA Bulletin 108, 545-561.

765 Grimm, G.W., Bouchal, J.M., Denk, T., Potts, A., 2016. Fables and foibles: A critical analysis of
766 the Palaeoflora database and the Coexistence Approach for palaeoclimate reconstruction. Rev.
767 Palaeobot. Palynol. 233, 216-235.

Grimm, G.W., Denk, T., 2012. Reliability and resolution of the coexistence approach - A revalidation using modern-day data. Review of Palaeobotany and Palynology 172, 33-47.

Grimm, G.W., Potts, A.J., 2016. Fallacies and fantasies: the theoretical underpinnings of the Coexistence Approach for palaeoclimate reconstruction. Climate of the Past 12, 611-622.

Hagen, E.R., Royer, D.L., Moye, R.A., Johnson, K.R., 2019. No Large Bias within Species between the Reconstructed Areas of Complete and Fragmented Fossil Leaves. Palaios 34, 43-48.

Hembree, D.I., Hasiotis, S.T., 2007. Paleosols and ichnofossils of the White River Formation of Colorado: insight into soil ecosystems of the North American Midcontinent during the Eocene-Oligocene transition. Palaios 22, 123-142.

Huber, M., Goldner, A., 2012. Eocene monsoons. Journal of Asian Earth Sciences 44, 3-23.

Huff, P.M., Wilf, P., Azumah, E.J., 2003. Digital Future for Paleoclimate Estimation from Fossil Leaves? Preliminary Results. Palaios 18, 266-274.

Jacobs, B.F., 2004. Palaeobotanical studies from tropical Africa: relevance to the evolution of forest, woodland and savannah biomes. Philosophical Transactions of the Royal Society of London, B, Biological Sciences 359, 1573-1583.

Keeley, J.E., 1999. Chaparral, in: Barbour, M.G., Billings, W.D. (Eds.), North American Terrestrial Vegetation, Second ed. Cambridge University Press, Cambridge, pp. 203-254.

Körner, C., 2013. Vegetation of the Earth, in: Bresinsky, A., Körner, C., Kadereit, J.W., Neuhaus, G., Sonnewald, U. (Eds.), Strasburger's Plant Sciences: Including Prokaryotes and Fungi. Springer-Verlag, Berlin, pp. 1217-1262.

Kowalski, E.A., Dilcher, D.L., 2003. Warmer paleotemperatures for terrestrial ecosystems. PNAS 100, 167-170.

Kunzmann, L., Moraweck, K., Müller, C., Schröder, I., Wappler, T., Grein, M., Roth-Nebelsick, A., 2019. A Paleogene leaf flora (Profen, Sachsen-Anhalt, Germany) and its potentials for palaeoecological and palaeoclimate reconstructions. Flora 254, 71-87.

Leopold, E.B., Clay-Poole, S., 2001. Florissant leaf and pollen floras of Colorado compared: Climatic Implications, in: Evanoff, E., Gregory-Wodzicki, K.M., Johnson, K.R. (Eds.), Fossil flora and stratigraphy of the Florissan Formation, Colorado. Denver Museum of Nature and Science, Denver, pp. 17-70.

Leopold, E.B., Liu, G., Clay-Poole, S., 1992. Low-biomass vegetation in the Oligocene?, in: Prothero, D.R., Berggren, W.A. (Eds.), Eocene-Oligocene Climatic and Biotic Evolution. Princeton University Press, Princeton, pp. 399-420.

Lielke, K., Manchester, S.R., Meyer, H.W., 2012. Reconstructing the environment of the northern Rocky Mountains during the Eocene/Oligocene transition: constraints from the palaeobotany and geology of south-western Montana, USA. Acta Palaeobotanica 52, 317-358.

Little, S.A., Kembel, S.W., Wilf, P., 2010. Paleotemperature Proxies from Leaf Fossils Reinterpreted in Light of Evolutionary History. PLoS ONE 5, 1-8.

Lloyd, K.J., Worley-Georg, M.P., Eberle, J.J., 2008. The Chadronian mammalian fauna of the Florissant Formation, Florissant Fossil Beds National Monument, Colorado, in: Meyer, H.W., Smith, D.M. (Eds.), Paleontology of the upper Eocene Florissant Formation, Colorado. Geological Society of America, Boulder, Colorado, pp. 117-126.

Lowe, A.J., Greenwood, D.R., West, C.K., Galloway, J.M., Sudermann, M., Reichgelt, T., 2018. Plant community ecology and climate on an upland volcanic landscape during the Early Eocene Climatic Optimum: McAbee Fossil Beds, British Columbia, Canada. Palaeogeography, Palaeoclimatology, Palaeoecology 511, 433-448.

MacGinitie, H.D., 1953. Fossil Plants of the Florissant Beds, Colorado. Carnegie Institution of Washington Publication 599, Washington, D.C.

MacGinitie, H.D., 1969. The Eocene Green River Flora of Northwestern Colorado and Northeastern Utah. University of California Press, Berkeley, California, USA

MacGinitie, H.D., 1974. An Early Middle Eocene flora from the Yellowstone-Absaroka Volcanic Province, northwestern Wind River Basin, Wyoming. University of California Publications in Geological Science, Berkeley, California, USA.

Manchester, S.R., 1989. Attached reproductive and vegetative remains of the extinct American-European genus *Cedrelospermum* (Ulmaceae) from the early Tertiary of Utah and Colorado. American Journal of Botany 76, 256-276.

Manchester, S.R., 2000. Late Eocene fossil plants of the John Day Formation, Wheeler County, Oregon. Oregon Geology 62, 51-63.

Manchester, S.R., 2001. Update on the megafossil flora of Florissant, Colorado, in: Evanoff, E., Gregory-Wodzicki, K.M., Johnson, K.R. (Eds.), Fossil flora and stratigraphy of the Florissant Formation, Colorado. Denver Museum of Nature & Science, Denver, pp. 137-161.

Manchester, S.R., Crane, P.R., 1983. Attached leaves, inflorescences, and fruits of *Fagopsis*, an extinct genus of fagaceous affinity from the Oligocene Florissant flora of Colorado, U.S.A. American Journal of Botany 70, 1147-1164.

Merkhofer, L., Wilf, P., Haas, M.T., Kooyman, R.M., Sack, L., Scoffoni, C., Cúneo, N.R., 2015. Resolving Australian analogs for an Eocene Patagonian paleorainforest using leaf size and floristics. American Journal of Botany 102, 1160-1173.

Meyer, H.W., 1992. Lapse rates and other variables applied to estimating paleoaltitudes from fossil floras. Palaeogeogr Palaeoclim Palaeoecol 99, 71-99.

Meyer, H.W., 2001. A review of the paleoelevation estimates for the Florissant flora, Colorado, in: Evanoff, E., Gregory-Wodzicki, K.M., Johnson, K.R. (Eds.), Fossil flora and stratigraphy of the Florissant Formation, Colorado. Denver Museum of Nature & Science, Denver, pp. 205-216.

839 Meyer, H.W., 2003. The Fossils of Florissant. Smithsonian Books, Washington.

840 Meyer, H.W., 2016. Forest responses to climate cooling across the Eocene-Oligocene boundary
841 in western North America, GSA Annual Meeting. Geological Society of America, Denver, CO,
842 pp. Paper No. 74-20.

843 Miller, I.M., Brandon, M.T., Hickey, L.J., 2006. Using leaf margin analysis to estimate the mid-
844 Cretaceous (Albian) paleolatitude of the Baja BC block. Earth and Planetary Science Letters 245,
845 95-114.

846 Mooney, H.A., Dunn, E.L., 1970. Photosynthetic systems of Mediterranean-climate shrubs and
847 trees of California and Chile. The American Naturalist 104, 447-453.

848 Mosbrugger, V., Utescher, T., 1997. The coexistence approach--a method for quantitative
849 reconstructions of Tertiary terrestrial palaeoclimate data using plant fossils. Palaeogeography,
850 Palaeoclimatology, Palaeoecology 134, 61-86.

851 Peppe, D.J., Baumgartner, A., Flynn, A., Blonder, B., 2018. Reconstructing Paleoclimate and
852 Paleoecology Using Fossil Leaves, in: Croft, D.A., Su, D., Simpson, S.W. (Eds.), Methods in
853 Paleoecology: Reconstructing Cenozoic Terrestrial Environments and Ecological Communities.
854 Springer International Publishing, pp. 289-317.

855 Peppe, D.J., Royer, D.L., Cariglino, B., Oliver, S.Y., Newman, S., Leight, E., Enikolopov, G.,
856 Fernandez-Burgos, M., Herrera, F., Adams, J.M., Correa, E., Currano, E.D., Erickson, J.M.,
857 Hinojosa, L.F., Hoganson, J.W., Iglesias, A., Jaramillo, C., Johnson, K.R., Jordan, G.J., Kraft,
858 N.L.B., Lovelock, E.C., Lusk, C.H., Niinemets, U., Penuelas, J., Rapson, G., Wing, S.L., Wright,
859 I.J., 2011. Sensitivity of leaf size and shape to climate: global patterns and paleoclimatic
860 applications. New Phytologist 190, 724-739.

861 Peppe, D.J., Royer, D.L., Wilf, P., Kowalski, E.A., 2010. Quantification of large uncertainties in
862 fossil leaf paleoaltimetry. Tectonics 29, 1-14.

863 Poorter, H., Niinements, U., Poorter, L., Wright, I.J., Villar, R., 2009. Causes and consequences
864 of variation in leaf mass per area (LMA): a meta-analysis. New Phytol 182, 565-588.

865 Prothero, D.R., 2008. Paleogene climates, in: Gornitz, V. (Ed.), Encyclopedia of
866 Paleoclimatology and Ancient Environments. Kluwer Academic Publishers, Dordrecht, The
867 Netherlands, pp. 728-733.

868 Reich, P.B., 1995. Phenology of tropical forests: patterns, causes, and consequences. Canadian
869 Journal of Botany 73, 164-174.

870 Reichgelt, T., Kennedy, E.M., Mildenhall, D.C., Conran, J.G., Greenwood, D.R., Lee, D.E.,
871 2013. Quantitative palaeoclimate estimates for early Miocene southern New Zealand: evidence
872 from Foulden Maar. Palaeogeogr Palaeoclim Palaeoecol 378, 36-44.

873 Retallack, G.J., 2007. Cenozoic Paleoclimate on Land in North America. The Journal of Geology
874 115, 271-294.

875 Roth, J.L., Dilcher, D.L., 1978. Some considerations in leaf size and leaf margin analysis of
876 fossil leaves. Courier Forschungsinstitut Senckenberg 30, 165-171.

877 Royer, D.L., Miller, I.M., Peppe, D.J., Hickey, L.J., 2010. Leaf Economic Traits from Fossils
878 Support a Weedy Habit for Early Angiosperms. American Journal of Botany 97, 438-445.

879 Royer, D.L., Peppe, D.J., Wheeler, E.A., Ninements, Ü., 2012. Roles of climate and functional
880 traits in controlling toothed vs. untoothed leave margins. American Journal of Botany 99, 915-
881 922.

882 Royer, D.L., Sack, L., Wilf, P., Lusk, C.H., Jordan, G.J., Niinements, U., Wright, I.J., Westoby,
883 M., Cariglino, B., Coley, P.D., Cutter, A.D., Johnson, K.R., Labandeira, C.C., Moles, A.T.,
884 Palmer, M.B., Valladares, F., 2007. Fossil leaf economics quantified: calibration, Eocene case
885 study, and implications. Paleobiology 33, 574-589.

886 Royer, D.L., Wilf, P., Janesko, D.A., Kowalski, E.A., Dilcher, D.L., 2005. Correlations of
887 climate and plant ecology to leaf size and shape: potential proxies for the fossil record. American
888 Journal of Botany 92, 1141-1151.

889 Schneider, C.A., Rasband, W.S., Eliceiri, K.W., 2012. NIH Image to ImageJ: 25 years of Image
890 Analysis. Nat Methods 9, 671-675.

891 Sheldon, N.D., Retallack, G.J., 2004. Regional paleoprecipitation records from the late Eocene
892 and Oligocene of North America. The Journal of Geology 112, 487-494.

893 Smith, D.M., 2000. The evolution of plant-insect interactions: Insights from the Tertiary fossil
894 record, Geosciences. The University of Arizona, Tucson.

895 Smith, D.M., 2008. A comparison of plant-insect associations in the middle Eocene Green River
896 Formation and the upper Eocene Florissant Formation and their climatic implications, in: Meyer,
897 H.W., Smith, D.M. (Eds.), Paleontology of the upper Eocene Florissant Formation, Colorado.
898 The Geological Society of America, Boulder, pp. 89-104.

899 Smith, G.A., Manchester, S.R., Ashwill, M., Mcintosh, W.C., Conrey, R.M., 1998. Late Eocene–
900 early Oligocene tectonism, volcanism, and floristic change near Gray Butte, central Oregon.
901 Geological Society of America Bulletin 110, 759-778.

902 Spicer, R.A., Valdes, P.J., Spicer, T.E.V., Craggs, H.J., Srivastava, G., Mehrotra, R.C., Yang, J.,
903 2009. New developments in CLAMP: Calibration using global gridded meteorological data.
904 Palaeogeography, Palaeoclimatology, Palaeoecology 283, 91-98.

905 Strömberg, C.A.E., 2005. Decoupled taxonomic radiation and ecological expansion of open-
906 habitat grasses in the Cenozoic of North America. Proceedings of the National Academy of
907 Sciences 102, 11980-11984.

908 Strömberg, C.A.E., 2011. Evolution of Grasses and Grassland Ecosystems. Annu. Rev. Earth
909 Planet. Sci. 39, 517-544.

910 Turner, I.M., 1994. Sclerophylly: primarily protective? Functional Ecology 8, 669-675.

911 Uhl, D., 2006. Fossil plants as paleoenvironmental proxies - some remarks on selected
912 approaches. Acta Palaeobotanica 46, 87-100.

913 Utescher, T., Mosbrugger, V., 2007. Eocene vegetation patterns reconstructed from plant
914 diversity — A global perspective Palaeogeogr Palaeoclim Palaeoecol 247, 243-271.

915 Veatch, S.W., Meyer, H.W., 2008. History of paleontology at the Florissant fossil beds,
916 Colorado, in: Meyer, H.W., Smith, D.M. (Eds.), Paleontology of the Upper Eocene Florissant
917 Formation, Colorado. Geological Society of America, Boulder, pp. 1-18.

918 Wappler, T., Labandeira, C.C., Rust, J., Frankenhäuser, H., Wilde, V., 2012. Testing for the
919 effects and consequences of mid Paleogene climate change on insect herbivory. PLoS ONE 7,
920 e40744.

921 Wilf, P., 1997. When are leaves good thermometers? A new case for Leaf Margin Analysis.
922 Paleobiology 23, 373-390.

923 Wilf, P., 2000. Late Paleocene-early Eocene climate changes in southwestern Wyoming:
924 Paleobotanical analysis. Geol Soc of Am Bull 112, 292-307.

925 Wilf, P., Labandeira, C.C., Johnson, K.R., Coley, P.D., Cutter, A.D., 2001. Insect herbivory,
926 plant defense, and early Cenozoic climate change. PNAS 98, 6221-6226.

927 Wilf, P., Wing, S.L., Greenwood, D.R., Greenwood, C.L., 1998. Using fossil leaves as
928 paleoprecipitation indicators: An Eocene example. Geology 26, 203-206.

929 Wing, S.L., Greenwood, D.R., 1993. Fossils and fossil climate: the case for equable continental
930 interiors in the Eocene. Philosophical Transactions of the Royal Society of London, Series B:
931 Biological Sciences 341, 243-252.

932 Wingate, F.H., Nichols, D.J., 2001. Palynology of the uppermost Eocene lacustrine deposits at
933 Forissant Fossil Beds National Monument, Colorado, in: Evanoff, E., Gregory-Wodzicki, K.M.,
934 Johnson, K.R. (Eds.), Fossil flora and stratigraphy of the Florissant Formation, Colorado. Denver
935 Museum of Nature & Science, Denver, CO, pp. 71-135.

936 Wolfe, J.A., 1971. Tertiary climate fluctuations and methods of analysis of Tertiary floras.
937 Palaeogeogr Palaeoclim Palaeoecol 9, 27-57.

938 Wolfe, J.A., 1972. An Interpretation of Alaskan Tertiary Floras, in: Graham, A. (Ed.), Floristics
939 and paleofloristics of Asia and eastern North America. Elsevier, Amsterdam.

940 Wolfe, J.A., 1979. Temperature parameters of humid to mesic forests of eastern Asia and
941 relation to forests of other regions of the northern hemisphere and Australasia. U.S. Geological
942 Survey Professional Paper 1106, 1-37.

Wolfe, J.A., 1992. An Analysis of Present-Day Terrestrial Lapse Rates in the Western Conterminous United States and Their Significance to Paleoaltitudinal Estimates. U.S. Geological Survey Bulletin 1964, 1-35.

Wolfe, J.A., 1993. A method of obtaining climatic parameters from leaf assemblages. U.S. Geological Survey Bulletin 2040, 73 pp.

Wolfe, J.A., 1994. Tertiary climatic changes at middle latitudes of western North America. Palaeogeography, Palaeoclimatology, Palaeoecology 108, 195-205.

Wolfe, J.A., Forest, C.E., Molnar, P., 1998. Paleobotanical evidence of Eocene and Oligocene paleoaltitudes in midlatitude western North America. GSA Bulletin 110, 664-678.

Wolfe, J.A., Spicer, R.A., 1999. Fossil leaf character states: a multivariate analyses, in: Jones, T.P., Rowe, N.P. (Eds.), Fossil Plants and Spores: modern techniques. Geological Society, London, pp. 233-239.

Wood, H.E., Chaney, R.W., Clark, J., Colbert, E.H., Jepsen, G.L., Reeside, J.R., Stock, C., 1941. Nomenclature and correlation of the North American continental Tertiary. Bulletin of the Geological Society of America 52, 1-48.

Wright, I.J., Reich, P.B., Cornelissen, J.H.C., Falster, D.S., Groom, P.K., Hikosaka, K., Lee, W., Lusk, C.H., Niinements, U., Oleksyn, J., Osada, N., Poorter, H., Warton, D.I., Westoby, M., 2005. Modulation of leaf economic traits and trait relationships by climate. Global Ecology and Biogeography 14, 411-421.

Yates, M.J., Verboom, G.A., Rebelo, A.G., Cramer, M.D., 2010. Ecophysiological significance of leaf size variation in Proteaceae from the Cape Floristic Region. Functional Ecology 24, 485-492.

Zaborac-Reed, S.J., Leopold, E.B., 2016. Determining the paleoclimate and elevation of the late Eocene Florissant flora: support from the coexistence approach. Can. J. Earth Sci. 53, 565-573.

Zachos, J.C., Dickens, G.R., Zeebe, R.E., 2008. An early Cenozoic perspective on greenhouse warming and carbon-cycle dynamics. Nature 451, 279-283.

Figure and Table Captions

Fig. 1. Location of Florissant Fossil Beds National Monument (FLFO) in central Colorado, U.S.A. The lower left map highlights the modern topography and major cities in Colorado. The small blue rectangle is enlarged in the lower right. The National Monument, shown in green, is near the western boundary of Teller County and just south of Route 24. The 24.3 km^2 National Monument is approximately 48 km west of Colorado Springs.

Fig. 2. The stratigraphic context of the middle shale unit of the Florissant Formation at Collection Site 9 in Florissant Fossil Beds National Monument, Colorado, U.S.A. **A.** Deep sea benthic foraminiferal oxygen isotope ratios ($\delta^{18}O$), highlighting Eocene-Oligocene cooling (~33 Ma) occurring just after deposition of the upper Eocene Florissant Formation (~34 Ma; dotted line), modified from Zachos et al. (2008). **B.** Generalized stratigraphy of the Florissant Formation and the underlying regional unconformity. The Florissant Formation consists of six informal units (lower shale, lower mudstone, middle shale, caprock conglomerate, upper shale, and upper pumice conglomerate). Radiometric dates ($^{40}Ar/^{39}Ar$ of sanidine) were obtained from several pumice samples taken from the arrowed positions, altogether averaging 34.07 ± 0.10 (Evanoff et al., 2001). Modified from Evanoff et al. (2001). **C.** Stratigraphic column of the middle shale unit at Collection Site 9. Lithostratigraphic units are labeled; fossil plants used in this study were sampled from those units labeled with an asterisk. Please note, the legend corresponds with panel C only.

Fig. 3. Overview of leaf diversity at Collection Site 9 used in the digital leaf physiognomy analysis from the middle shale unit in Florissant Fossil Beds National Monument, Florissant, Colorado, U.S.A. The proportion of untoothed vs. toothed-margined taxa displayed here is nearly identical to that of the entire site. **A.** Morphotype 2, cf. *Cotinus,* FLFO 10088A **B.** Morphotype 3, *Caesalpinites acuminatus,* FLFO 10297 **C.** Morphotype 5, *Athyana haydenii,* FLFO 6678B **D.** Morphotype 7, *Carya libbeyi*, FLFO 10392 **E.** Morphotype 9, *Cercis parvifolia,* FLFO 6172 **F.** Morphotype 12, *Fagopsis longifolia,* FLFO 11167B **G.** Morphotype 14, *Populus crassa,* FLFO 11240B **H.** Morphotype 17, *Quercus* cf. *scottii,* FLFO 10843B **I.** Morphotype 18, *Rhamnites pseudo-stenophyllus,* FLFO 10576B **J.** Morphotype 19, *Rhus stellariaefolia,* FLFO 10244A **K.** Morphotype 22, *Amelanchier scudderi,* FLFO 6664A **L.** Morphotype 24, FLFO 11463 **M.** Morphotype 25B, *Salix ramaleyi,* FLFO 8591A **N**. Morphotype 26, *Sapindus coloradensis,* FLFO 10002A **O.** Morphotype 29, *Ulmus tenuinervis,* FLFO 11085B **P.** Morphotype 30, *Vauquelinia coloradensis,* FLFO 8963A **Q.** Morphotype 32, *Hydrangea fraxinifolia* / *Staphylea acuminata,* FLFO 10578B **R.** Morphotype 33, *Cedrelospermum lineatum,* FLFO 10023B **S.** Morphotype 34, cf. *Quercus,* FLFO 10539A **T.** Morphotype 37, *Acer florissanti,* FLFO 10822A **U.** Morphotype 38, cf. *Colubrina spireaefolia,* FLFO 6832 **V.** Morphotype 41, FLFO 11057B **W.** Morphotype 43, *Quercus peritula,* FLFO 8572A **X.** Morphotype 48, FLFO 6627 **Y.** Morphotype 53, FLFO 6369A **Z.** Morphotype 57, cf. *Daphne septentrionalis,* FLFO 11128 **AA.** Morphotype 58, FLFO 10966B **BB.** Morphotype 59, FLFO 11037A **CC.** Morphotype 68, FLFO 11320. Specimens are housed in the collection of Florissant Fossil Beds National Monument

(FLFO). Images courtesy of the National Park Service, photographed by FLFO Staff. Scale bars = 10 mm.

Fig. 4. Leaf mass per area distributions of Florissant leaves ($N \geq 1$) compared to modern floras from different biomes and depositional environments. Modern leaf mass per area data from Peppe et al., (2011). Leaf mass per area is grouped into bins of 20 $g \cdot m^{-2}$. **A.** Florissant fossil assemblage with distributions for all morphotypes ($N \geq 1$) and those with $N > 1$. **B.** Pee Dee State Park, South Carolina, USA. **C.** Buena Vista, Puerto Rico. **D.** Connecticut River, near Middletown Connecticut, USA. **E.** Barro Colorado Island, Panama. **F.** Half Moon Bay, California, USA. **G.** Placerville, California, USA.

Fig. 5. Physiognomy of Florissant leaves (orange) plotted among all sites used in the digital leaf physiognomy calibration dataset (blue). Modern seasonally-dry forests of Australia that have distinctly low Feret's diameter ratios, similar to Florissant, are highlighted with blue shading. Two sites in Tasmania are noted for their particularly close correspondence to Florissant. Number of teeth : internal perimeter is the ratio of the number of teeth to the perimeter of the leaf after the teeth are removed.

Fig. 6. Distributions of measured leaf teeth variables for taxa which could be confidently aligned with those ascribed to riparian and non-riparian vegetation types by Bouchal et al. (2014) using NLR inference. *P* values calculated from a Student's t-test, unequal variance, one-tailed. See Table S2 for additional detail. **A.** Perimeter ratio, i.e., the ratio of the perimeter before teeth are digitally moved (external) to the perimeter after they are removed (internal). **B.** The number of teeth per internal perimeter.

Table 1. Leaf mass per area (M_A) estimates per taxon.

Table 2. Comparison of mean annual temperature and site averaged leaf mass per area estimates (M_A) for several Eocene sites.

Table 3. Temperature and precipitation estimates from this study.

Table 4. Previously published temperature estimates for the late Eocene Florissant flora using leaf physiognomic and nearest living relative approaches.

Figure

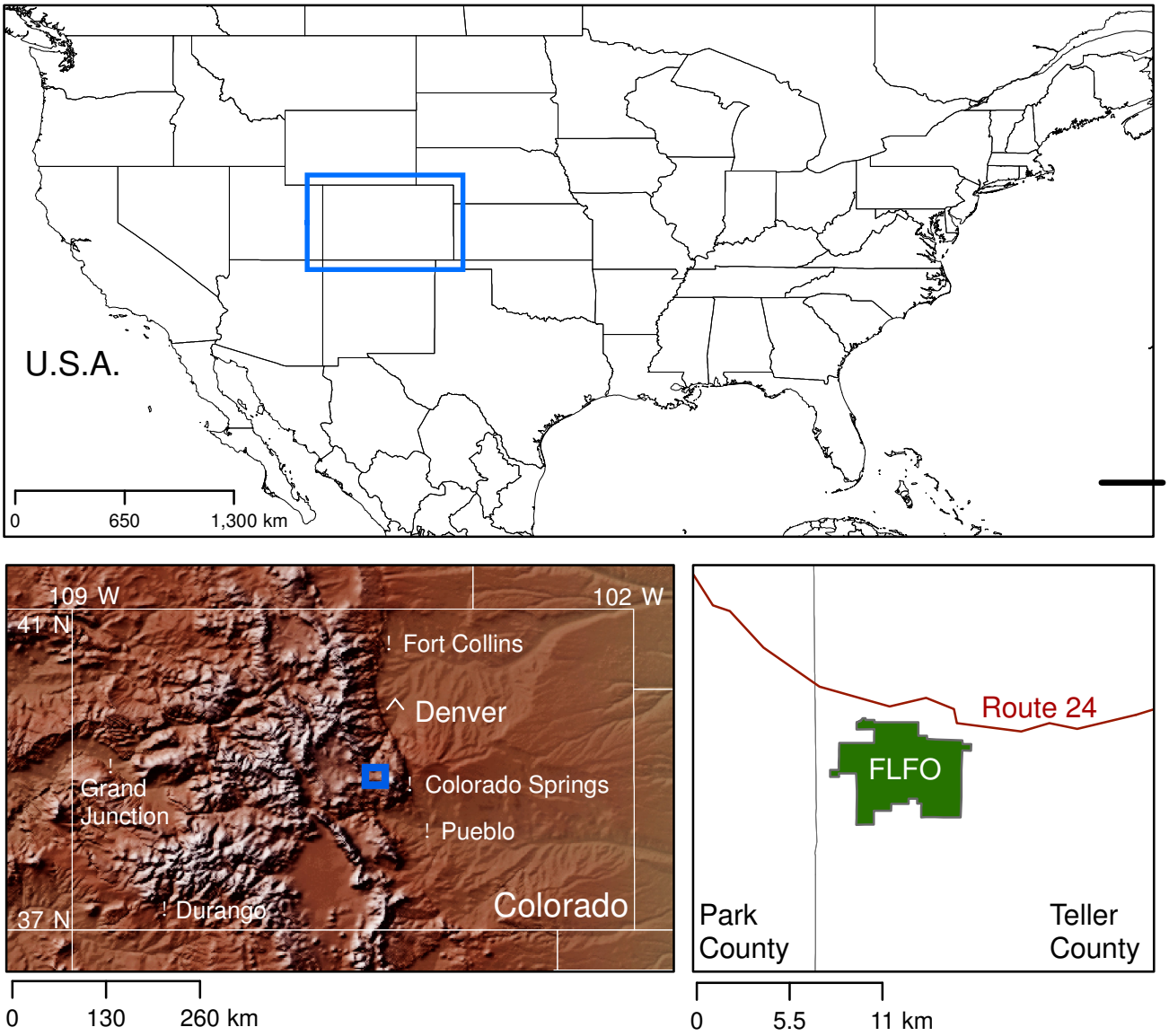

Figure 1

Figure

Click here to access/download;Figure;Allen et al_Fig 2_Florissant DiLP.tif

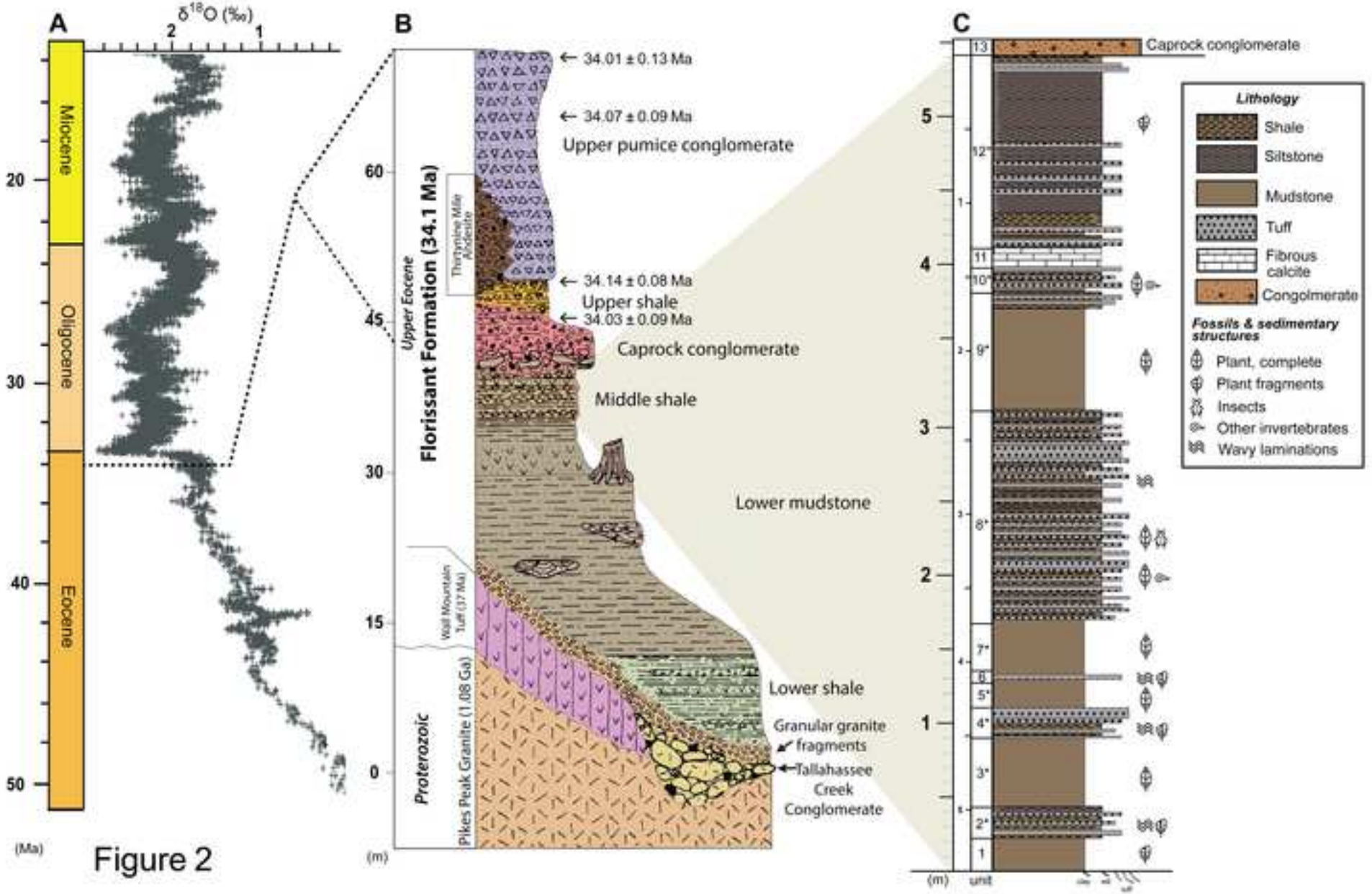

Figure 2

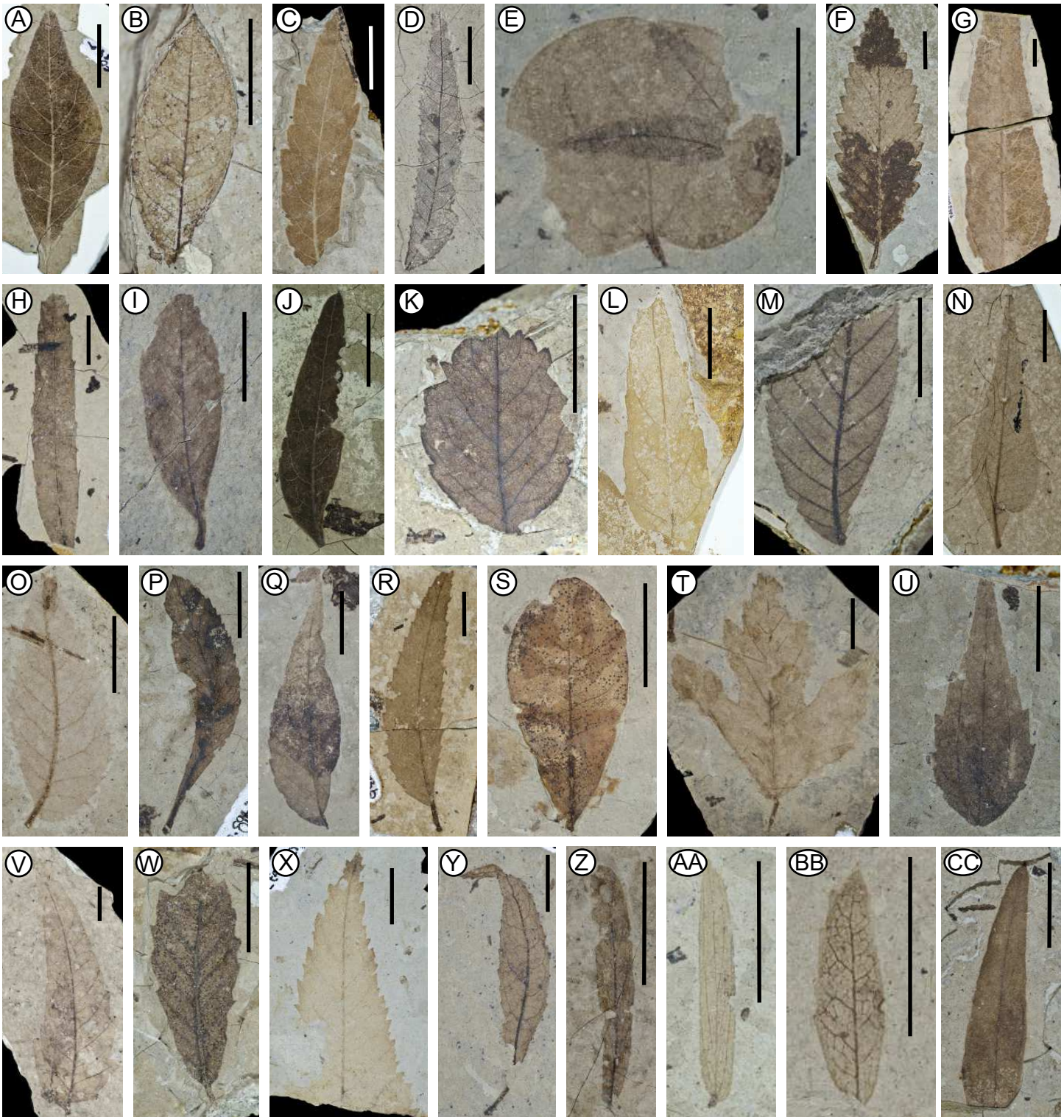

Figure 3

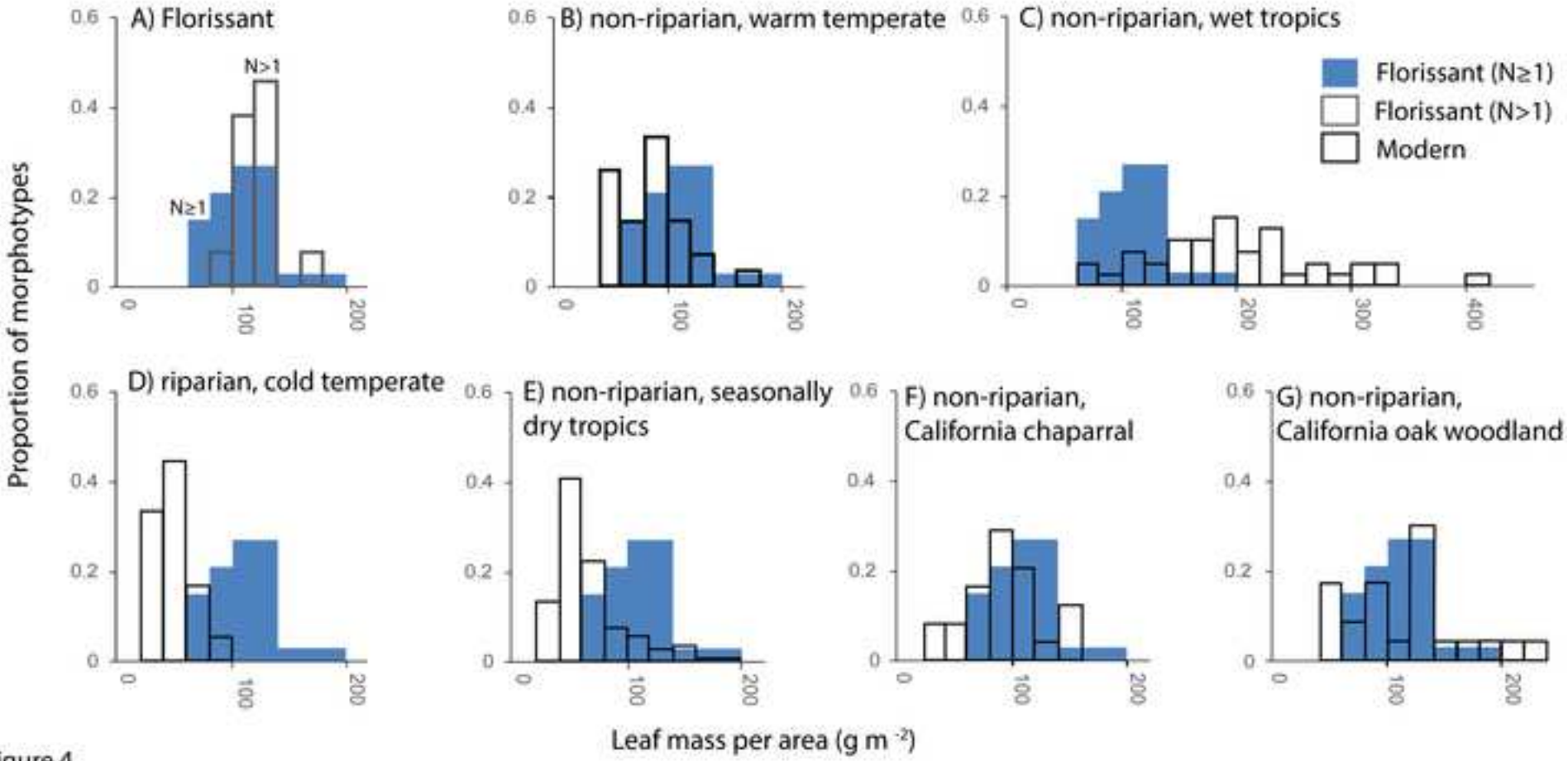

Figure 4

Figure

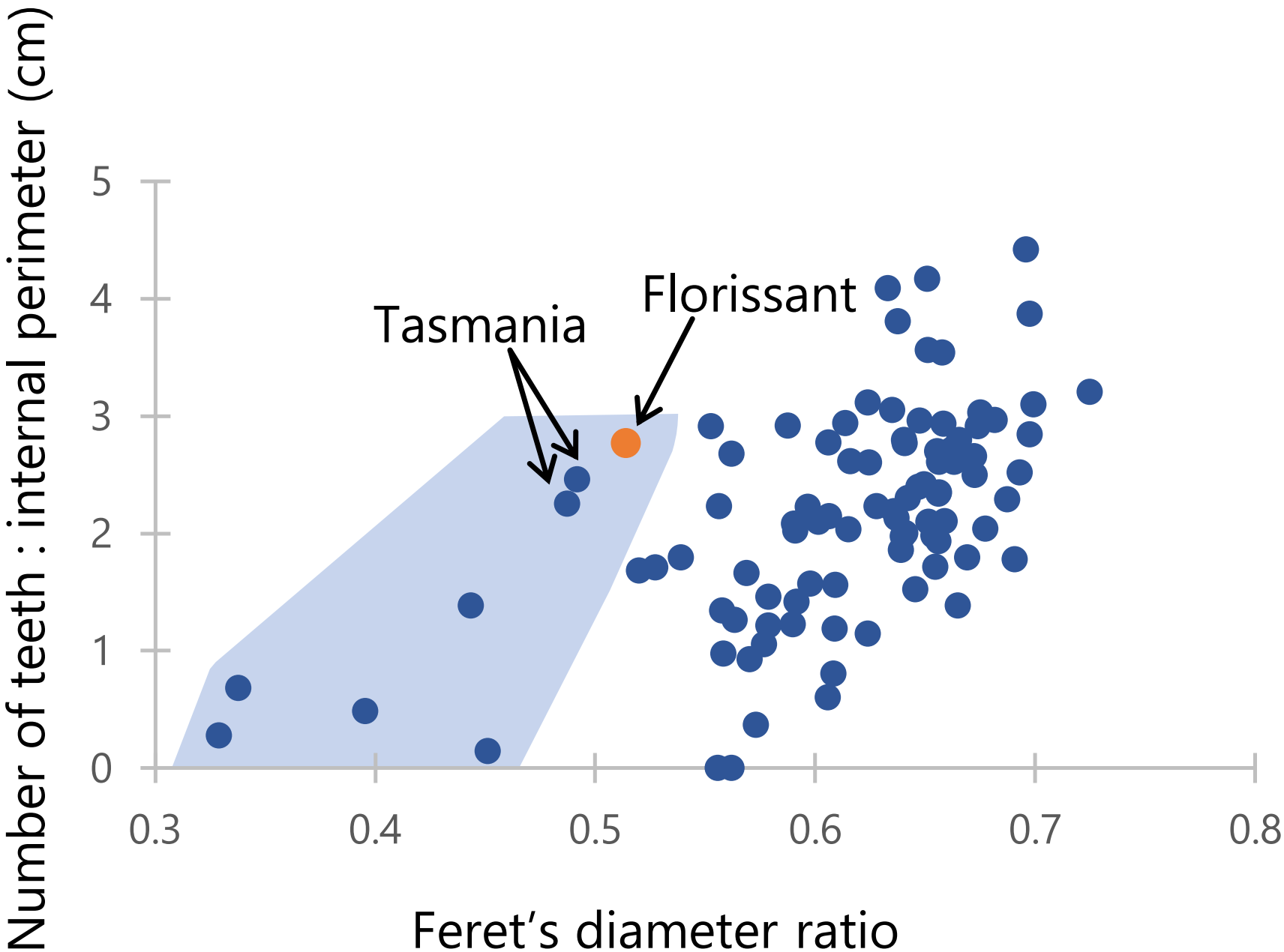

Figure 5

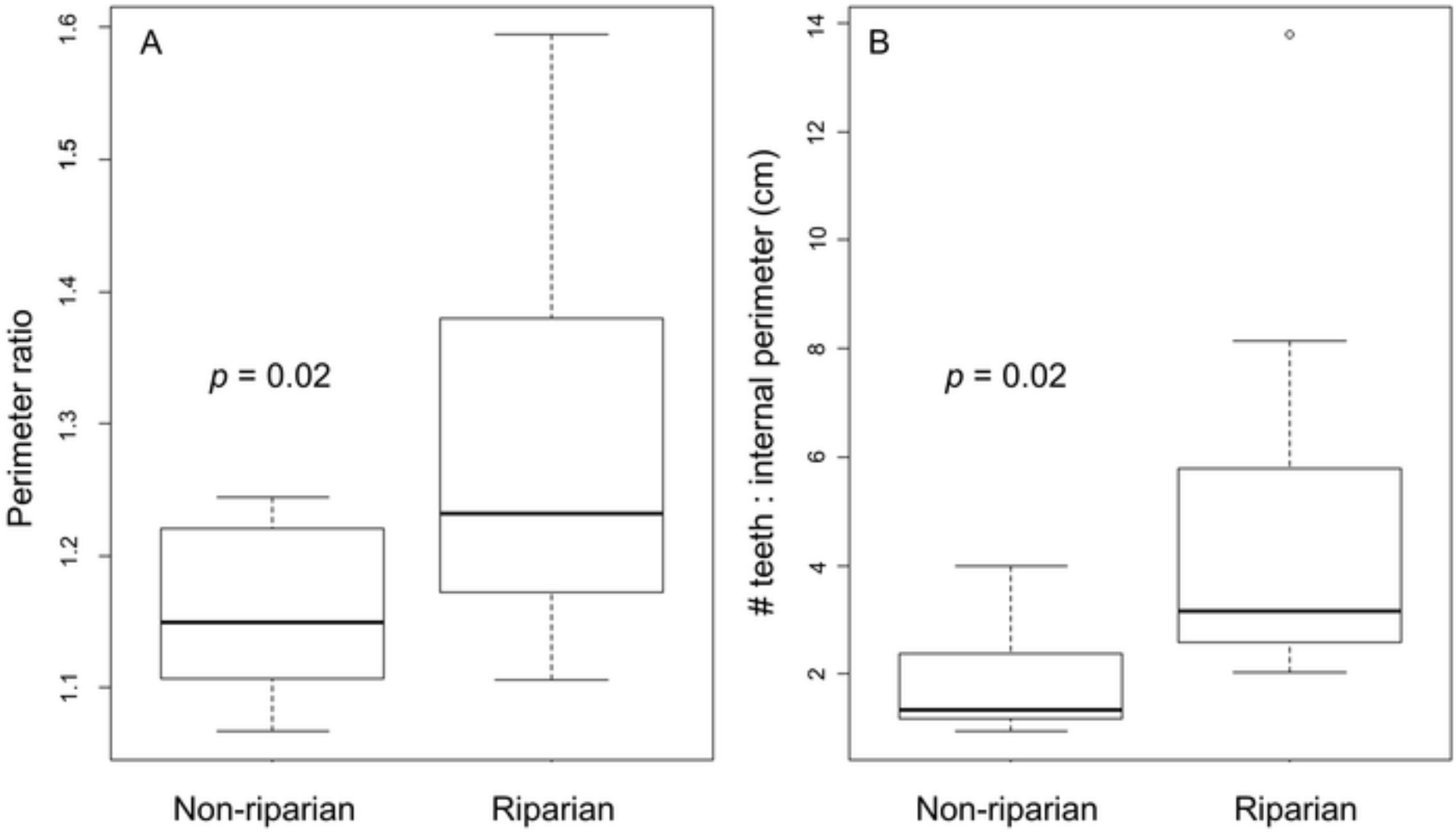

Figure 6